Identifying and analyzing spatial and temporal patterns of lightning-ignited wildfires in Western Canada from 1981-2018.

by

Olivia SR Aftergood

A thesis submitted in partial fulfillment of the requirements for the degree of

Master of Science
in
Forest Biology and Management

Department of Renewable Resources

University of Alberta

Abstract

This study looked at the spatial and temporal patterns of lightning-ignited wildfires in Western Canada from 1981 to 2018. Studying these sequences are of great importance as wildfires have had serious implications on communities, forests, and provide operational issues for fire managers. Moreover, with climate change which is predicted to affect these arrangements could in turn exacerbate these conflicts. To assess distribution patterns over space and time, the nearest neighbors, K-function, Mann-Kendall and the Getis-ord Gi* statistics were employed. All lightning attributed wildfires recorded within Western Canada (Alberta, Saskatchewan, Manitoba, British Columbia, Yukon, and the Northwest Territories) in the Canadian National Fire Database were used in this analysis, where statistics were performed in R and ArcGIS. Results suggest that lightning-ignited wildfires are spatially clustering on the Western Canadian landscape up to 270 km with an observed overall non-significant decreasing trend seen for NOF (number of fires). Moreover, hotspot areas, where lightning fires are showing a trend increase and or are clustering spatially over the 37-year period, are displayed in GIS. Although determining factors that cause the reoccurrence of spatial and temporal clustering are widely speculated, a result of climate and vegetation could be the main influences of these patterns, however, further research needs to be undertaken. Wildfires are becoming a force to be reckoned with in an earth influenced by anthropogenic climate change. Ecological disasters are on the rise, communities are being afflicted, and costly disaster bills are increasing. Understanding lightning fires and their distributions within space and time is crucial in quantifying their extents on the Canadian landscape and how this interaction is being altered. Further research needs to be undertaken to better understand these mechanisms so fire managers can be better equipped in dealing with wildfires in a changing climate.

Acknowledgements

The completion of this research and thesis work would not have been possible without the supportive team that I had throughout this journey. The greatest appreciation is to my supervisor, Dr. Mike Flannigan who was a constant wealth of knowledge and a great mentor throughout my entire research. It was a pleasure to have worked with you in a capacity for development, learning and guidance, thank you! To my committee members, Mike Flannigan and Mike Wotton as well as my defence examining committee member Charles Nock, it was a pleasure to interact with you and thank you for all your feedback on this project.

I would also like to thank Dr. François Robinne who supported me with all things GIS related, to Dr. Sean Coogan, thank you for all your guidance, discussions, and humour. To Xinli Cai who helped me with my project, R and provided the CFS data. To the students of the fire lab, Jessica Zerb, Andrew Stack, Rodrigo Campos, Kyle Elliot, Kiera Stewart, and everyone else thank you for your love and support. To my supportive roommates, Kate Beezoyen and Hilary Cameron, thank you. I could not have gotten through this rollercoaster without your support, comfort, and laughter. To Miriam Mahaffy, a wonderful friend who was such a rock for me during this journey. I would also like to thank my astounding cheer team and family, Margot, David, Sarah, Jonathan and Luna for being my biggest fans, a huge support system as they were always their for me with their continuous love, support, and belief in my academic achievements.

Thank you to the University of Alberta and staff in the Department of Renewable Resources in providing support through every stage of my research. The Canadian Partnership for Wildland Fire Science and The University of Alberta for providing the funding for this research.

Table of Contents

List of Tables

List of Figures

List of Abbreviations

AB	Alberta
BC	British Columbia
BUI	Built up Index
CG	Cloud-to-ground
CFFDRS	Canadian Forest Fire Danger Rating System
CSR	Complete Spatial Randomness
CWFIS	Canadian Wildland Fire Information System
°C	Degrees Celsius
DC	Drought Code
DMC	Duff Moisture Code
FFMC	Fine Fuel Moisture Code
ft	Feet
FWI	Fire Weather Index
ha	Hectares
Hexel	Hexagon
ISI	Initial Spread Index
kA	Kiloampere
km	Kilometer
LCC	Long continuing current
MB	Manitoba
Mha	Millions of hectares
mm	Millimetres
m/s	Meters per second
NN/ANN	Nearest Neighbour/Average Nearest Neighbour
NOF	Number of Fires
NWT	Northwest Territories
RH	Relative Humidity
Sd	Standard Deviation
SK	Saskatchewan
US	United States
Western Canada	Provinces of AB, BC, SK, MB and territories of YK and NWT
WUI	Wildland Urban Interface
YK	Yukon

Chapter 1

Introduction

1.1 Context

Wildfires have the potential to be an integral ecological disturbance within biological communities (Rowe 1983); this can be a result from either human induced fire or from an environmental interaction between a lightning strike and vegetation. Studies looking in Australia, North and Central America and Europe date plant adaptations in fire-prone environments back to the early Paleocene (Crisp et al. 2011; He et al. 2012), this evolution of the fire-vegetation cycle has created multiple fire-adapted traits in vegetation as a result of this interaction (Pausas and Keeley 2014). Moreover, this type of disturbance mechanism positively influences species richness, diversity, and habitat quality (Thom and Seidl 2016) however, anthropogenic climate change is altering this relationship.

Climate change is transforming the climatic conditions (i.e. temperature, precipitation, and relative humidity) an ecological community experiences. This is resulting in rates of change in ecosystems being faster than species can adapt too (IUCN 1990). An example of the effects of climate change concerning wildland fires, is the theorized increases of lightning strike densities which have the potential to increase fire frequencies on the landscape in North America (Romps et al. 2014). Another example discusses vegetation composition altering due to fire and climate conditions, where certain species are no longer supported by their environment thereby altering species migration within these affected areas (Veraverbeke et al. 2017; Hart et al. 2019). Moreover, changes in the climate can create variable fuel moisture content in the vegetation through less precipitation which leads to severe drought conditions that impacts forest resilience (Wotton and Flannigan 1993; Flannigan et al. 2000a; Stocks et al. 2000; Coogan et al. 2018).

These small cumulative changes occurring because of climate change can be highlighted, especially in recent years as the destructive capacity of wildfires on communities and infrastructure has increased. In 2016, the Horse River fire in Fort McMurray, Alberta caused extensive damage to the community where it is considered one of the largest natural and costliest disasters in Canada. It resulted in insured losses around $3.58 billion dollars (The Conference Board of Canada 2017). Fire managers and communities are faced with difficult decisions about mitigation, prevention and protection of communities and values of interest. Furthermore, it is difficult to quantify and fully understand the patterns of lightning and lightning-ignited wildfires on a forested landscape and how climate change is affecting these patterns.

Therefore, this thesis addresses two questions.

(1) Do lightning-ignited wildfires exhibit distribution patterns over space and time on the Western Canada landscape, between 1981-2018, and

(2) Characterize the spatial and temporal distribution of lightning fires by;

i) examining specific locations of high and low values exhibiting clustering between 1981-2018,

ii) examining trends associated with these high and low values,

iii) examining distances (km) of clustering occurring in the data,

iv) examining these high and low values when looking at different months from 1981-2018.

1.2 Wildland fire in Canada

As a dominant ecological disturbance in Canada's boreal forest, fire has historically been generated from humans and the natural process of lighting (Rowe and Scotter 1973; Rowe 1983; Weber and Flannigan 1997). While these long withstanding fundamental interactions, which has been definitively shaping and impacting a community's ecological health and resilience (Thom and Seidl 2016), hasn't always been realized at the forefront in fire management. The 1871 Wisconsin and Michigan fires that killed over 1500 people sparked the first misconceptions of fires role in forests. Wildfires became perceived in these forested communities as destructive, this prompted fire policy into adopting intensive management practices and fire exclusion principles from the landscapes (Oberle 1969). It also spurred research concerning wildland fire science to quantify and understand the mechanisms fueling wildfires. Fire initiation requires heat, oxygen and fuel (Countryman 1972; Pyne et al. 1996; Moritz et al. 2005). Fire behaviour, which describes a wildland fires flame development, fire initiation and spread, is described by the fire environment concept. This concept considers the elements of fuel, weather and topography to be ruling a fire's behaviour (Countryman 1972). In addition to these factors, one can evaluate a fire regime to fully understand and assess the impacts a wildfire is having on a given landscape. The concept of a fire regime describes how fires interacts with an ecosystem through space and time. The elements used to describe a fire regime are fire frequency, fire type, fire size, seasonality, fire intensity, fire severity, and ignition source (Malanson 1987; Merrill and Alexander 1987; Weber and Flannigan 1997; Sommers et al. 2011). These elements are defined below: Fire frequency is the number of fires based on spatial and temporal factors; Fire type refers to where a fire is burning in the stand: (a) ground, (b) surface, (c) crown; Fire size describes the amount of area a fire has burned in units such as hectares (acres); Seasonality considered the time of year a fire occurs, fire intensity is the amount of energy released in kW/m;

Fire severity is the amount of fuel consumed in kg/m^2; Ignition source references the cause of a fire start which can either be human or lightning (Malanson 1987; Weber and Flannigan 1997; Flannigan et al. 2000a; Stocks et al. 2000; Stocks et al. 2003; Sommers et al. 2011; Hanes et al. 2019).

In Canada, the average annual area burned is 2 million ha, with some years experiencing up to 7 million ha. A small portion, roughly ~3% of all wildland fires in Canada that exceed beyond 200 ha account for ~97% of the area burned (Stocks et al. 2003), this small percentage of fires are widely attributed to lightning starts and therefore account for the majority of area burned (Stocks et al. 2003; Coogan et al. 2018; Hanes et al. 2019). This is mostly due to remote fires that are not easily accessible, detected and actioned (Stocks et al. 2003). Lightning and lightning-ignited wildfires in Canada are an integral component when studying wildfire science. Lightning regulates the length of a fire season and it determines when an area will see fire on a landscape in space and time (Van Wagtendonk and Cayan 2010).

In Canada, a nationwide system was developed and adopted to predict fire danger ratings, fire indices and fire intensities, it is called the Canadian Forest Fire Danger Rating System (CFFDRS) and a subsystem, the Canadian Forest Fire Weather Index (FWI) system (Van Wagner 1987; Stocks et al. 1989; Taylor et al. 1996). The FWI system is strictly weather based and reliant on four weather inputs: (1) noon local standard time (LST) weather observations of temperature, (2) 24-hour precipitation, (3) relative humidity, and (4) 10 m wind speed. This system generates codes that provide a broad outlook of fuel moisture and expected fire behaviour for an area if initiation were to occur. Three of the indices detail the moisture content of the top, middle, and bottom layers of fuel on the forest floor, they are the fine fuel moisture code (FFMC), the duff moisture code (DMC), and the drought code (DC), respectively. The other

indices are indicators of the rate of fire spread (the initial spread index, ISI), the amount of fuel available to burn/depth of burn (the build-up index, BUI), and the fireline intensity (the fire weather index, FWI) (Van Wagner 1987).

As mentioned above, wildfire is integral in ecological communities, however conflict between fire and humans has been documented since the early 1800s and is only becoming ever more apparent within the coming years. Canada has been significantly affected by wildfires; the province of British Columbia burned over 1 million hectares of forest in 2017 and in 2018 and cost approximately just over $600 million for both years (Government of British Columbia 2020). The province of Alberta suffered extensive damage and fire suppression costs during the Fort McMurray (2016) and Slave Lake (2011) wildfires (The Conference Board of Canada 2017). Research conducted by Stocks and Martell in 2016, stated that fire management costs nation-wide were on the rise. Expenditures in Canada increased from ~$300 million in 1970 to ~$900 million in 2013. This rise in costs can be attributed to Canada's primary practice of heavy suppression and fire exclusion on the landscape through aggressive resource deployment, referenced as initial attack (Wotton et al. 2010). This strategy is employed in part due to the continued expansion of the wildland-urban interface; this refers to an area where infrastructure or homes are inter-dispersed between wildland vegetation, and when a fire threatens or destroys these structures it is considered as a wildland-urban interface fire (Johnston and Flannigan 2018). As human development maintains its expansion into forested areas (e.g. urban/rural sprawl and industrial expansion) (Radeloff et al. 2005; Campos-Ruiz et al. 2018; Johnston and Flannigan 2018), stakeholders will only increase the pressure on fire managers and governments to prioritize suppression activities. This in turn has the potential to heighten management costs as protecting these values from a wildfire threat require a greater number of resources (Stocks and

Martell 2016). This dilemma will only amplify in the face of climate change, another problem fire managers face today.

Climate change is predicted to change the way fire interacts on a landscape. Lightning strike densities are predicted to increase (Romps et al. 2014), longer fire seasons are theorized (Wotton and Flannigan 1993), and an overall increase in extreme fire weather is indicated (Jain et al. 2017). These concepts and findings are especially important as the ecological framework that determines the spatial and temporal extents of lightning will shift as climate change increases its breadth on the earth's natural systems (Romps et al. 2014; Veraverbeke et al. 2017; Coogan et al. 2018). This has a potential to critically challenge provincial and national fire agencies and management practices and strategies due to more fire being realized on the landscape (Stocks and Martell 2016). To understand the repercussions of a changing environment one must recognize and explore the foundational interactions of fire with its forested environment. Therefore, lightning is an important component in comprehending how climate change is influencing fire on the landscape as it is a main driver of area burned. Furthermore, greater insight and research into lightning and its spatial-temporal patterns in Canada could provide valuable information for fire managers and researchers. It could aid in identifying hotspot regions within Canada that are susceptible to increases in lightning activity and area burned while highlighting vulnerable communities.

1.3 Lightning

A thunderstorm is a naturally occurring weather phenomena created by the interaction between moisture in the air, atmospheric instability, and a lifting agent. Thunderstorms are extremely variable and all exhibit geographical variations most efficiently explained through the environmental conditions (ex. atmospheric conditions) they experience (Flannigan et al. 2000b; Todd et al. 2000; Cooray 2014).

Lightning is an active electrical discharge created by the interaction between positive and negative charges in clouds (Latham and Williams 2001). Strikes are categorized by their polarity; polarity is the positive or negative nature of a lightning strike. When water droplets rise they can collide with particles of ice in the cloud, the particles that have freezing droplets are negatively charged. This process is more likely to occur and therefore an excess amount of negatively charged ions occur, due to the dipole the positive and negative ions separate resulting in positive ions being pulled to the top half of the cloud and the negative ions situating at the lower sections of the cloud (Fuquay 1982). This process generates lightning. It was summarized that for North America, specifically the United States that roughly 90% of lightning strikes are negative and 10% are positive strikes (Uman 1985). For the entirety of Canada between 1999-2008 it was found that positive strikes comprised of 12-35% of strikes in northern regions and 7-15% of strikes in the summer (Burrows and Kochtubajda 2010). There are two predominant types of lightning: intracloud lightning (IC) and cloud-to-ground lightning (CG). Intracloud lightning is a discharge contained completely within the cloud that connects the negative and positive charges. A cloud-to-ground (CG) strike is an ionized path where ions (positive or negative) travel between the cloud and ground (Latham and Williams 2001).

Typically these strike channels can exceed temperatures of 50,000°F (27,760°C), voltages exceeding 200 kA with a median of 33 kA, velocities between 10-30% that of the speed of light and are on average 5-12 km long (Hileman 1999). Multiplicity is the number of return strokes in a flash of lightning; these strokes are current surges discharged during the lightning strike (Kochtubajda and Burrows 2010). A flash of lightning experiences between 1 to 54 strokes; the average is 3 strokes per flash (Hileman 1999). In Canada, it was recorded that the monthly average stroke for negative strikes in the summer months between 1999-2008 was between 2-2.4 strokes (Burrows and Kochtubajda 2010). Negative lightning strikes are considered to have one to several return strokes, while positive lightning strikes more commonly exhibit only one (Fuquay et al. 1967; Fuquay 1982; Kochtubajda and Burrows 2010). There is evidence that lightning-ignited wildfires are caused primarily by long continuing currents (LCC) (Fuquay et al. 1967; Fuquay et al. 1972; Podur et al. 2003). Long continuing currents are when the stroke experiences a continuous discharge over a relatively long period of time (Latham and Williams 2001), roughly 4 to 542 m/s (Saba et al. 2006). Positive lightning strikes have shown to have a higher probability to exhibit LCC (Fuquay et al. 1967; Fuquay 1982; Flannigan and Wotton 1991; Saba et al. 2006; Kochtubajda and Burrows 2010; Van Wagtendonk and Cayan 2010), and are therefore considered to be a main characteristic in starting wildfires. Kochtubajda and Burrows (2010) found that flashes with peak currents >100 kA accounted for ~0.9% of flashes in Canada between 1999-2008 and mostly were positive strikes. Van Wagtendonk and Cayan (2010) found that in California 40% of the negative strikes seen had some type of long continuing current. Flannigan and Wotton (1991) called attention to the fact that negatively charged lightning occurs in greater frequencies and therefore its relationship with LCC needs greater consideration. Moreover, they state that not every LCC will result in a wildfire and

therefore great uncertainty exists concerning what characteristics of lighting are linked to wildfire initiation.

There are three types of thunderstorms: single-cell, multi-cell clustering, and supercells. For air-mass thunderstorms which are typically single-cell storms, the thunderstorm can travel anywhere between 38 – 63 km/h, have a life span of roughly 5 to 25 mins (Liu and Li 2016), and cover an area of ~170 km^2 dependent on month and climatic conditions. When looking at lightning strike densities, more updrafts are associated with higher discharge activity because it can bring the electrically charged particles higher. Although this happens with all three thunderstorm types, supercells and multi-cell thunderstorms are bigger and cover larger areas; thereby allowing more electrical conditions to take place in the cloud resulting in higher strike counts (Meyer et al. 2013).

Another important aspect about lightning is dry lightning, dry lightning is defined for the United States as when 0.3 mm/h or less of precipitation is seen within a 72 to 96 h period after a lightning strike. However, this is regional dependent and therefore varies as Northeastern United States regions consider dry lightning to be 0.8 mm/h or less within a 2-3 days period (Vant-Hull et al. 2018). Ultimately, all these lightning characteristics need to be considered when looking at the effects of lightning-caused fire occurrences in forested areas as many variables play a role in wildfire initiation (Flannigan and Wotton 1991; Ordóñez et al. 2012).

1.4 The non-randomness of lightning and lightning-ignited wildfires

Multiple studies have investigated the spatial aspects of lightning; it has been found that lightning and lightning-ignited fires tend to cluster spatially on the landscape (Vázquez and Moreno 1998; Vázquez and Moreno 2001). Podur et al (2003) found that wildfires aggregated in spatial cluster sizes of around 150-200 km in Ontario, Canada. Another analysis by Genton et al (2006) in Florida, found that wildfires occurred in spatial cluster groups starting at 2 km and up. Research by Wang and Anderson (2010) established that lightning-ignited wildfires in Alberta, Canada clustered spatially in groups between 50 to 130 km. Furthermore, Masrur et al (2018) highlighted that between 2001 and 2015 wildfires in the circumpolar Arctic bioclimatic subzones (Yukon, Northwest Territories, Alaska, Greenland, and Russia) exhibited spatial and temporal clustering. This study focused primarily on the temporal scale and looked at three different scales, (a) 15-year time scale, (b) Aggregation of data between May-October per analysis year, (c) Monthly analysis. Overall, these studies demonstrate that lightning attributed wildfires are clustering spatially and temporally on the landscape.

However, uncertainty exists concerning specific variables that are influencing the spatial and temporal distributions. Several variables are mentioned in the literature and are considered to have merit in wildfire clustering; examples of these variables are mesoscale circulations (Dissing and Verbyla 2003), major land-water boundaries (Orville et al. 2002), fuel moisture constrained by dead and down fuel size as well as forest type (Renkin and Despain 1991), anthropogenic factors (Parisien et al. 2006), drought (Meyn et al. 2010), diurnal heating and cooling cycle (Burrows and Kochtubajda 2010).

Although multiple elements are proposed, there are some considered to be some major factors controlling these spatial and temporal patterns. Podur et al (2003), highlighted elevation

as a factor in ignition probability in Ontario, Canada, while Reap (1991), established that there was a positive relationship between lightning strike density and elevation below 800 m (2,624 ft) in Alaska. Hileman (1999), expressed limitations of whether lightning can occur at altitudes above 18,000 ft (5486.4 m), and Van Wagtendonk (1993), conducted a spatial analysis of lightning-ignited fires in Yosemite National Park that concluded elevation played a role in lightning and wildfire distributions. It was found that the highest percent of strikes occurred between 9000 and 10, 000 ft (2,953 and 3,281 m). Moreover, the largest portion of wildfires occurred at an elevation between 7,000 and 8,000 ft (2,297 and 2,625 m).

Despite this, topography and local terrain features need to also be considered as they shape the local country which can affect the local elevation within different forested communities. Topography is suspected to influence convective activity (thunderstorm development) through differential heating (Dissing and Verbyla 2003). Topography also plays a role in influencing and altering substrate, topo climate and vegetation (Genet et al. 2013) as well as drainage, fuel moisture and vegetation growth (Mundo et al. 2013) which all affect wildfire initiation. Likewise, it is suspected that elevated local terrain features play a role in the spatial distribution of strike density (Orville et al. 2002). Lightning activity has been impacted and highly retailored by local terrain features, elevation, and diurnal heating (Burrows and Kochtubajda 2010).

Yet, one can look at longitudinal variation as another aspect limiting lightning distribution between the north-south extents of North America (Orville et al. 2002). Morissette and Gauthier (2008) found significant differing spatial distribution in Quebec, Canada for lightning strike densities between the north-south and east-west gradients. They detail that strike density is higher in the south and western sections of their study area, highlighting that the strike

densities coincided with longitudinal and latitudinal gradients. In addition, Larjavaara et al (2005) detected a strong north-south gradient of lightning-ignited wildfire densities in Finland.

Vegetation is an additional component that needs to be considered. Van Wagtendonk and Cayan (2010), found that bioregions were a great tool in organizing and distinguishing between the spatial patterns of lightning-ignited wildfires in California. They determined that strike densities were most prevalent in mountainous and desert regions. Within mountainous terrain, lightning was associated with forests that produce heavy fuel loads. Wierzchowski et al (2002), found that the ecoregions of the Cordillera and Interior Plains showed substantial variation in lightning and lightning-ignited wildfires in Canada. They found that in British Columbia, only 50 strikes were required to start one wildfire compared to Alberta's 1400 strikes to one wildfire. This led to the suggestion British Columbia displays a high degree of spatial overlapping of lightning fire occurrence. They surmised that the primary variables associated with resulting in lightning-ignited wildfires were elevation, a severity rating, lightning strike distributions, and vegetation compositions. One study theorized that there is a higher ignition probability associated with certain vegetation types depending on their foliage cast (Latham and Williams 2001). This is emphasized in Renkin and Despain (1991), that saw 34% of their forest study area in Yellowstone NP which consists of mature spruce-fir, Douglas-fir and older stands of lodgepole pine, accounted for where roughly 60% of lightning-caused fires occurred. Krawchuk et al (2006), identified that forest composition played a factor in influencing lightning-ignited wildfires in Alberta, Canada. They detected that the probability of ignition was greater in spruce dominated landscapes as opposed to deciduous forests. Vegetation is considered to differ in terms of its fire intensity seen because each forest type has different characteristics associated with a fuel type. These various traits affect how a stand burns; some examples of these traits are

the foliar moisture content of a stand particularly between spring and summer, crown base height of a typical stand, understory growth and crown bulk densities (Wagner 1977).

Besides vegetation, climate is a major variation controlling spatial extents of lightning-caused fires. Reap (1991), suggested that the formation of thunderstorms in Alaska were a result of large-scale static instability from local wind and moisture. Dissing and Verbyla (2003), established that most lightning-ignited wildfires are initiated by localized air mass thunderstorms in Alaska. These storms are driven by mesoscale properties that all influence convection. Examples of these properties are albedo, surface roughness, sensible heat flux, and topography. Larjavaara et al (2005), observed that Finland experiences differences between its southern and northern ranges in terms of wildfires seen in the regions, which could be attributed to climate-caused variations in fuel moisture and lightning probability. Krawchuk et al (2006), detected that weather conditions played an extensive role in lightning-ignited wildfires in the boreal forests of Alberta, Canada. It was determined that weather (fuel moisture conditions) explained a large proportion of the variation in the ignition probability. Wang and Anderson (2010), identified that lightning-ignited wildfires in Alberta were further influenced by thunderstorms, mainly air mass thunderstorms. Landscapes and their associated fire regimes can be regulated by various factors such as regional climates, landscape variations in physiography and ecosystem structures (Kasischke et al. 2010). Veraverbeke et al (2017), constituted that for the Northwest Territories and Alaska, tree cover and climate variables (temperature, precipitation, and convective precipitation) explained 56 % of the spatial variability for lightning density. Specifically, 68% of the spatial variance of lightning density in Alaska is due to the interactions between the climate and tree cover; suggesting that surface energy fluxes from the forest influence the probability of lightning. All in all, climatic conditions play a major role in wildfire initiation and have a large-

scale influence on a magnitude of associated variables. In Canada, climatic variables are easiest documented and recorded as part of the Canadian Forest Fire Danger Rating (CFFDRS) System, specifically the subsystem of the Fire Weather Index (FWI) System. This is due to that fact that the four primary inputs of the FWI system are temperature, precipitation, wind, and relative humidity (Van Wagner 1987). Flannigan and Wotton (1991), summarized that the DMC is one of the most important indicators in explaining lightning-ignited forest fires in northwestern Ontario, Canada. Podur et al (2003), found that elevation and a DMC exceeding 20 were factors in ignition probability in Ontario, Canada. It was determined that higher DMC and FFMC values result in higher fire occurrences leading to the conclusion that drought conditions in the top layers of soil influence the number of lightning-ignited wildfires that are realized on a landscape (Krawchuk et al. 2006; Portier et al. 2019). As a result, using the indices and codes calculated from the FWI system can be a useful tool in determining wildfire initiation.

1.5 Climate change

Climate change and its associated impacts have been a concern for researchers for decades. This concern stems from the fact that a climate an ecosystem experiences controls its structures and systems; and the rate at which the climate is changing due to anthropogenic forces is unprecedented and unquantified (Wotton and Flannigan 1993; Weber and Stocks 1998; Stocks et al. 2000). Multiple studies have analyzed and depicted the potential impacts forests could experience in an environment influenced by climate change. Price and Rind (1994) estimated that in a 2 x CO_2 climate change scenario, the US could see the annual mean lightning fires increase by 44% and the mean annual area burned increase by 78%. Weber and Stocks (1998), stated that all projected climate scenarios concerning the boreal forest generally predicted a warmer, drier environment leading to longer fire seasons and increased fire severity due to the fuels being directly impacted. They also highlighted the lack of understanding and uncertainty around carbon storage and soil-plant relations in a changing ecosystem.

Research by Flannigan et al (2000a), highlighted the impact climate change could have on the ecosystems of the United States by increases in area burned, fire intensity and severity, thereby shifting the fire regime. Another study by Weber and Flannigan (1997), proposed that the far-reaching impacts of climate change on the boreal forest systems and functions could be astronomical due to the unprecedented rate at which the climate is shifting. This is because fire behaviour responds quickly to changes in weather components. Gillett et al (2004), determined that Canada had experienced increases in area burned over three decades since 1970. This trend is likely a result of warming temperatures during the fire season that could be attributed to anthropogenic greenhouse gases and sulfate aerosol emissions over the last eighty years. Alaska has also seen increases in the frequency of large fire years. This is especially visible during the

late-season; leading to higher rates of burning due to large extreme fire events in remote areas that are too massive to control (Kasischke et al. 2010). Flannigan et al (2016), indicated that increases in temperature will lead to drier fuels which will allow fuels to become more receptive to ignition and sustain more vigorous fire spread. In addition, to combat this dryness an even greater amount of precipitation would be needed to offset the overall effects of climate change. Specifically, an increase in precipitation by 15% is needed to offset each subsequent 1°C rise in temperature. Another study by Wotton et al (2017), found similar results of increases of drier fuels and fire behaviour in the future starting from 2020 to the end of the century. Moreover, they found that crown fires were more likely to occur, leading to days where higher fire intensities could be experienced causing problems and exceeding suppression capabilities. Portier et al (2019), identified that fire size and fire occurrence is regulated by soil moisture which is highly sensitive to temperature shifts. However, as climate change intensifies it will continue to modify and reshape the spatial extents of lightning thereby effecting climates, fire regimes and wildfires on the landscape (Whitman et al. 2015).

Hanes et al (2019), established that in Canada area burned has been on the rise since 1959; this increase has been primarily observed in Western Canada where there has been increases in large lightning-ignited fires. Veraverbeke et al (2017), predicted that lightning frequency and convective storm activity will increase in North America by the mid twenty-first century. In recent years higher records of lightning-ignitions have been observed and evidence has pointed to higher instances of lightning-ignited fires in the northern boreal forest (Veraverbeke et al. 2017; Coogan et al. 2018). Romps et al (2014), surmised that with each 1 °C global-mean of warming, lightning strike densities will increase by 12%. Whitman et al (2015), summarized that ignition cause, burn severity and fire size are highly driven by climate.

As climate change continues to alter the environment, biophysical changes aren't the only concern. It is theorized that changes in moisture conditions have the potential to lead to higher rates of escaped fire from suppression efforts, resulting in fire agencies unable to manage and cope with suppression demands in the future (Portier et al. 2019). Suppression resources may reach their threshold for effectiveness leaving values at risk to destruction from wildfires. This will require a need to develop and consider alternative management methods, if not, then fire managers and their agencies may face crisis management when dealing with fires in the face of a changing climate (Wotton et al. 2017). As the need for more suppression and management becomes apparent, funding and monetary constraints will be limiting and difficult for fire operations (Mitsopoulos et al. 2016). Ultimately, as the climate continues to be affected and change its ecosystems functions and structure it can render ecological communities and urban areas vulnerable to wildfires events. This reshaping of fire regimes and how fire interacts on the landscape is key in understanding how to adapt for the needs of research, management, and policy.

1.6 Research Objective

This study looks to answer two questions: (1) Do lightning-ignited wildfires exhibit distribution patterns over space and time on the Western Canada landscape, between 1981-2018, and (2) Characterize these spatial and temporal distributions of lightning fires by; i) Examining specific locations of high and low values exhibiting clustering, ii) Examining trends associated with these high and low values, iii) Examining distances (km) of clustering occurring in the data, iv) Examining these high and low values when looking at different months of the year?

Chapter 2

Data and Methods

2.1 Study Area

This study was performed in the forested areas (~ 4,370,205 km^2) of the provinces of British Columbia, Alberta, Saskatchewan, Manitoba, the Territory of the Yukon, and the Northwest Territories referred to hereafter as Western Canada (*Figure 2.1*). This study region was chosen in part due to research by Hanes et al (2019) that found significant trends in total area burned, number of large fire events and number of lightning-caused wildfires (≥ 200 ha) to be increasing in the western provinces and territories of Canada. This piqued an interest in wanting to investigate further in Western Canada concerning wildfire. Moreover, selecting June, July and August for the seasonal component in this study was due to Coogan et al. (2018) that found lightning fires (≥ 2 ha) peak during June, July and August, as well as trends in the number of lightning fires increased by ecozones.

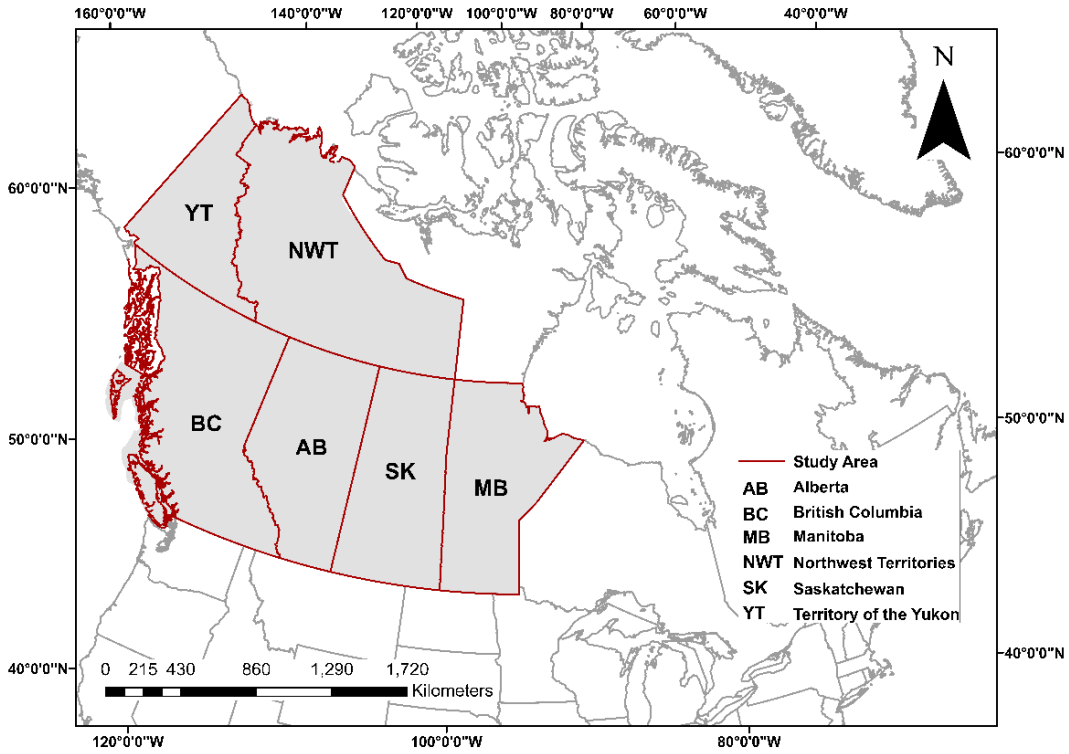

Figure 2.1 Outline of the study area comprised of all provinces and territories considered.

2.2 Data

Wildfire Data

The wildfire point data used in this research was obtained from the Canadian National Fire Database (Canadian Forest Service 2020) and assorted as follows. All wildfire points that were attributed to either human and or unknown causes were excluded from the analysis. Therefore, only lightning caused wildfires were looked at, moreover only point data occurring between 1981 to 2018 were included in the analysis. We further subdivided the data by only considering wildfires that occurred between April 1st – September 30th as is considered the official wildfire season in the majority of western provinces of Canada (Government of Alberta 2020; Government of British Columbia 2020). Moreover, the months of June, July and August

were analyzed as Coogan et al (2018) found increases in trends for lightning fires in those months within their study. This was also found in the data analyzed, where many lightning fires considered (~95 %) in this analysis occurred within these three months throughout the entire study period (*Figure 2.2).*

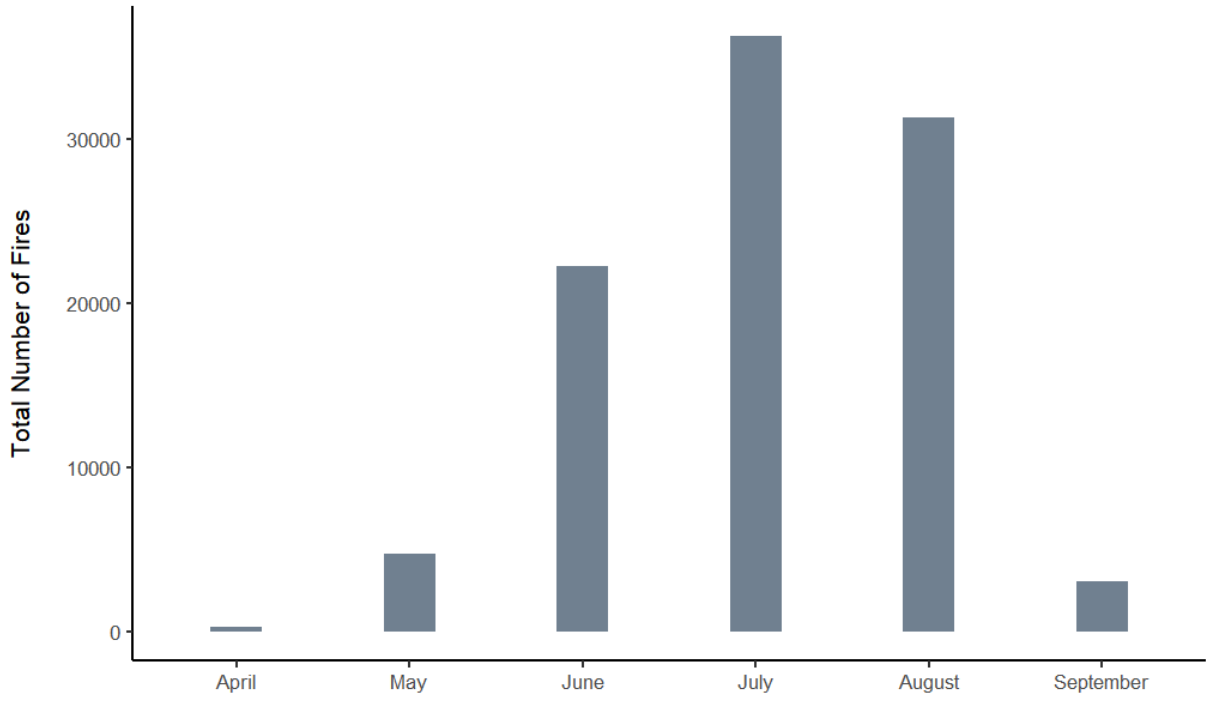

Figure 2.2 The total number of lightning caused wildfire points separated by month from 1981-2018 for Western Canada.

Only point data was analyzed and all wildfire points within the specific constraints of our study (i.e. Time period and seasonal component) were considered. A thing to note, we did not disqualify points from our study based on area burned as other studies have done, such as Hanes et al (2019) and Robinne et al (2016) who only considered data points (wildfires) that burned more than 200 ha, and Coogan et al (2018) who only considered data points (wildfires) that burned more than 2 ha. Therefore, a total of 97,921 points were analyzed and considered a

large enough data set to provide valuable and representative results. For these reasons, this analysis will only consider the number of fires (NOF). All point data within the prairie ecozone was not considered in this analysis, it was excluded due to the highly altered habitat within this region of large farm and croplands as well as human settlements (Robinne et al. 2016).

Table 2.1 The total number of lightning caused fire data points based on their area burned from the Canadian National Fire Database, between 1981-2018 and between April to September in Western Canada.

Area burned	Number of data points
All	97,921
> 2ha	24,084
> 200 ha	7,633

Some limitations to note, the Canadian national fire database is a compilation of provincial and territorial data into one centralized dataset; the lack of one uniform system has let to inherent data quality issues especially concerning older wildfire records. These older records as well as lightning-caused fire records possess inconsistencies due to under or lack of reporting from the fires occurring in northern or remote areas (Stocks et al. 2003). Furthermore, the classification of lightning-ignited wildfires may not be as accurate, this is due to mislabeled fires and therefore inflation and or deflation of data can occur (Podur et al. 2003; Stocks et al. 2003; Larjavaara et al. 2005; Bridge et al. 2005; Hanes et al. 2019). It has been indicated that data reported for fires under 200 ha are subjected to complications surrounding accuracy and inconsistency between different fire zones due to their differing policies and fire management practices (Bridge et al. 2005). Even with these caveats, this research is concerned about wildfire initiation on the landscape and therefore looking at the entire dataset is and can be valuable in provide details about the spatial and temporal patterns of lightning fires on the landscape.

2.3 ArcGIS Spatial and Temporal Analysis

Spatial data has inherent data quality issues associated with it, especially when conducting spatial analysis. These errors include issues in accuracy, scope, quality, and consistency; however, statistical analysis can eliminate or dampen these issues. Furthermore, major advances have occurred within recent years to improve data quality. Some of these advances have been undertaken in spatial data programs (Devillers et al. 2010) and are discussed below. This study looks to use a spatial data program, ArcGIS 10.7 (ESRI 2020) to conduct spatial analysis.

How to analyze spatial patterns

There are multiple issues and concerns about spatial data when conducting spatial analysis. An important concept to discuss when conducting research is scale. Scale is defined as a function of both extent and grain. Grain is considered the highest quality of spatial resolution that can be obtained within a given dataset. Extent is the size of the study area or the time of the study period (Turner et al. 2001). To determine an appropriate scale to use, consideration of one's research goals and objectives need to be assessed. The objectives of this thesis are: (1) Do lightning-ignited wildfires exhibit distribution patterns over space and time on the Western Canada landscape, between 1981-2018, and (2) Characterize these spatial and temporal distributions of lightning fires by; i) Examining specific locations of high and low values exhibiting clustering, ii) Examining trends associated with these high and low values, iii) Examining distances (km) of clustering occurring in the data, iv) Examining these high and low values when looking at different months of the year?

There is an inherent link between lighting, climate, and lightning-initiated wildfires. There are finer (*i.e.* small) scale climatic conditions that influence weather patterns and

connectivity. However, this research looks to conduct a study over a large area and time-period in the hopes to capture larger spatial and temporal patterns of lightning-ignited wildfire. This is considered a broader scaled (*i.e.* large) approach; a broad scale is defined as encompassing a larger area to provide a more generalized spatial analysis of the desired study landscape (Pearson 1993; Turner et al. 2001). The modifiable areal unit problem, first mentioned by Openshaw and Taylor (1979), outlines two major issues when spatial data is aggregated over space. The first concern is about zone sizes, as you change the size and shape of your zone your observed pattern changes. This indicates that models are scale dependent, meaning that a model applied at one scale may not be suitable at another scale therefore changing the observed spatial pattern seen (Lloyd 2014). The second issue is known as the ecological fallacy, this references issues that arise when making inferences about the nature of individuals from the groups those individuals are a part of (Robinson 1950). This concerns our study as this can produce misinterpretations of the results about individuals when looking at landscape spatial scale events, and therefore maintaining the same scale for all the data and analysis is crucial. To account for this bias, multiple regression (Turner et al. 2001) can be employed as well as Moran's *I* (Moran 1950) to test for spatial autocorrelation of the data. Although there are more tools out there to test for bias, creating and striving for robust results in terms of the data's sensitivity to changes in shapes and sizes of zones is also key (Lloyd 2014). It was summarized well by Openshaw (1977) when discussing solutions to this problem that spatial zones need to be able to represent both mapping of a model on to the data and vice versa. This can create a robust model overcoming fundamental spatial scale-dependent issues.

To deal with the spatial scale issues stated above within ArcGIS 10.7 (ESRI 2020), all point data was aggregated into a hexagon vector layer. The hexagon shape was employed as it is

less ambiguous than rectangles and provides a better visualization of the data. Hexagons are less ambiguous by provide a foundational platform for visual understanding and education about large amounts of synthesized data (Bodzin and Anastasio 2006), while also when computing cluster statistics, a hexagon models the data dispersal more accurately due to its shape (Birch et al. 2007). Therefore, extensive pre-analysis was conducted to determine the optimal grain (hexel) size to be used to create a robust and best fitting model. In order to determine an accurate hexel size, finding a compromise between the loss of information due to averaging while also representing adequate environmental variability is vital (Parisien et al. 2011; Robinne et al. 2016; Johnston and Flannigan 2018).

Hexagon

For the purposes of this analysis, each hexagon (hereafter hexel) contains a 30 km-width (77900 ha) and all hexagons together generated a hexagon vector grid (*Figure 2.3*) using the tool "Repeating shapes for *ArcGIS*" (Jenness 2012). This sized hexel was found to provide more robust results when considering the broad-scaled approach of the study during the exploratory analysis phase. Spatial data preparation and analysis was done using ArcGIS 10.7.1 (ESRI 2020) and R 3.1.1 (Team 2005).

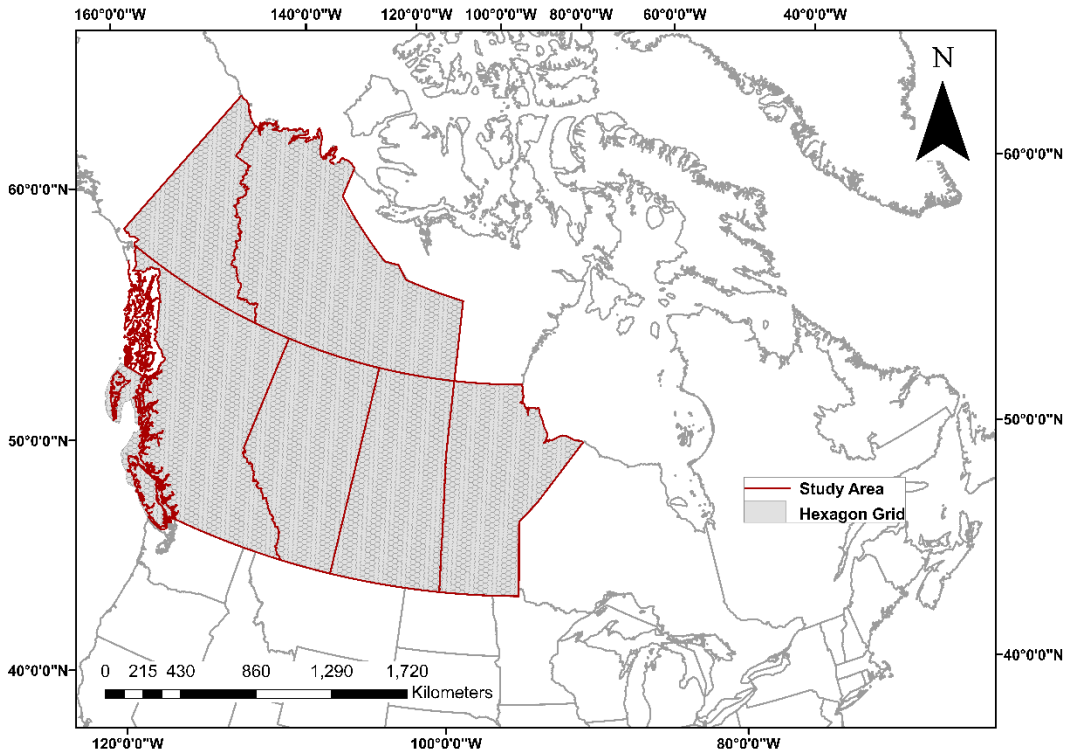

Figure 2.3 Location of study area overlaid with hexagon grid used in analysis

All data was projected using the Canada Lambert Conformal Conic coordinate system. Two types of maps are produced using two different data mining toolkits in ArcGIS. The optimized hotspot analysis which is based on the Getis-ord Gi* statistic, and the space-time data mining toolbox with the Space-Time Cube and the Emerging Hotspot analysis tools is based on both the Getis-Ord Gi* and the Mann-Kendall statistic. These two analyses are described as follows.

Optimized Hotspot Analysis

A hexagon grid was created for each study year with each hexel containing a centroid. Moreover, a hexagon grid was created for each analysis year for the months of June, July, and August. Then all the lightning fire data points were segregated by year and or month and each

year/month was spatially joined to the hexagon layer based on the aggregation of point counts per hexel. A distance band limit of 120 km was added to limit the k-means neighboring function between adjacent polygons; this was done to limit overfitting of data to the model. A distance band limit of 120 km was chosen as air-mass thunderstorms cover roughly 170 km^2 (Liu and Li 2016). This provided the basis of the analysis for the hotspot tool which analyzed each hexel and created a map that shows hexels in the 99^{th} %, 95^{th} %, and 90^{th} % for significant clustering based on a z-score and p-value. All maps are displayed by their z-score computed.

Space-Time Cube & Emerging Hotspot Tool

All wildfire point data was inputted into the aggregate space-time cube to create a file used in the emerging hotspot analysis. The space-time cube counts each data point per hexel per year and stores it in a cube where it determines the counts of points in each hexel over the study period. The emerging hotspot tool is used where it computes the Getis-Ord Gi* to determine hot and cold hexels and the Mann Kendall statistic looks at the Getis-Ord Gi* z-scores and determine whether the hexel trends are increasing or decreasing. Maps are then generated that exhibit hexel clustering and trend statistic z-scores which are displayed by the st. deviation. Moreover, a space-time cube and emerging hotspot analysis was created for each analysis year for the months of June, July, and August.

2.4 Spatial Statistics

This thesis follows several previous studies that have looked at and analyzed spatial-temporal point and polygon processes. A spatial-temporal point process is a random collection of points, where each point represents an event in space and time. These spatial-temporal point processes are referred to as spatio-temporal point patterns (Genton et al. 2006). A spatio-

temporal analysis can look at both space and time within non-point data, such as polygons (Delmelle et al. 2013). This study will look at both point patterns and non-point analysis of lightning wildfire ignitions in Western Canada, which consists of 97,921 wildfire points between the period of 1981-2018.

Podur et al (2003) analyzed spatial patterns of lightning-initiated wildfires in Ontario, Canada using spatial point statistical methods. They applied the statistical tool of the K-function to detect spatial dependence and the kernel estimation to study the distributions of lightning fires. Furthermore, the kernel estimation provided a visual presentation of the clustering pattern within the data. Genton et al. (2006) also analyzed spatio-temporal patterns of lightning and human wildfire ignitions in Florida using spatial point statistics. They used the nearest-neighbors statistic and the K and L-functions. Wang and Anderson (2010) looked at spatial and temporal distributions of lightning and human caused forest fires in Alberta from 1980-2007. They employed the K-function, L-function, and the kernel estimate of intensity. The K and L-functions can assess the distribution patterns of the data, while the kernel estimate can generate maps of estimated spatial intensity. They identified hotspots in Alberta through the kernel estimates of locations where human or lightning fires occur frequently. Coogan et al (2018) used 90%, 95% and 99% confidence interval thresholds for their analysis as well as the median to evaluate their trends in the data. Moreover, they used the Mann-Kendall statistic to evaluate trends in the data for human and lightning-caused wildfires >2 ha from 1981-2018. Jain et al (2017) also used the Mann-Kendall statistic with the Theil-Sen slope to assess trends in the data in the context of extreme fire weather and fire season length. Hanes et al (2019) looked at area burned and NOF in Canada using the Mann-Kendall trend statistic to test for possible serial correlation in the data and they used a bootstrap hypothesis test for significance. Masrur et al (2018) looked at

circumpolar spatial and temporal patterns of wildfire activity in the Arctic tundra from 2001-2015. They analyzed the spatial patterns of the data by employing the spatial tools of clusters/hotspot, spatial outliers (Moran's I) and spatial association (LISA autocorrelation measures) in ArcGIS 10.7 (ESRI 2020). They also looked at temporal patterns using correlation and regression statistics at three temporal scales, (a) 15-year period, (b) 6-month periods, (c) monthly periods. Robinne et al (2016) looked at area burned in Alberta, Canada in ArcGIS 10.7 (ESRI 2020) using hexels to display their biophysical model (in s.d. units) and area burned.

This research looks to build on these spatio-temporal patterns and point process statistics used, and looks to apply this to Western Canada, a larger spatial analysis over a longer temporal period (1981-2018). We looked to analyze point patterns as well as conduct broader (hexel) spatial statistics to detect lightning-initiated wildfire patterns.

A typical data analysis establishes its study with a test for complete spatial randomness (CSR), coupled with thereafter modelling the lack of spatial randomness. The nearest-neighbors statistic and the Kinhom(r) k-function were used, which tests a data's spatial distribution. The Getis-Ord Gi* allows you to visually present the spatial components of the data, while the Mann-Kendall trend statistic provides insight into the temporal trends of the data. In ArcGIS 10.7 (ESRI 2020), the optimized hotspot tool (Getis-ord Gi* statistic) and the space-time cube (Getis-ord Gi* and Mann-Kendall statistic) maps provide a visual pattern of the spatial and temporal features of the data. Moreover, the Moran I tool was used to test for spatial autocorrelation of the data. These statistics are discussed in-depth below.

(A)Spatial Point Pattern Statistics

K-Function

The K-function is a spatial descriptive statistic used to detect deviations from spatial homogeneity at different scales. K-function is defined as the number of extra points within distance *t* of a point calculated as follow (Dixon 2002):

$$K(t) = \lambda^{-1} E(.)$$

where λ is the density (mean number of points per unit area), *E*(.) is the expected value of the number of extra points within distance *t* of a randomly chosen event. Because this data is inherently spatial and evaluating the spatial model is key, employing the function *L*(t) to test complete spatial randomness (CSR) the Ripley's K-function (Dixon 2002), edge effect is used. The Ripley's edge correction was used to account for the bias associated with function and the shape of the study area. L(t) function is defined as:

$$\hat{L}(t) = [\hat{K}(t)/\pi]^{1/2}$$

Under CSR, $L(t) = t$. To show clustering, one can graph *L(t)* against *t*. Because incident point data of lightning-ignited wildfires are being analyzed for their spatial pattern at various distances and spatial scales, patterns vary, indicating the importance of spatial processes at work. Therefore, the inhomogeneous K-function was used to account for the spatial interaction of the point pattern (interpoint interactions) due to the data sets non-parametric properties. The inhomogeneous K-function, Kinhom(*r*) is a generalization of the "ordinary" K-function and the bootstrap confidence bands for the summary function was calculated to provide a lower and upper confidence band. The equation is defined as follows (Baddeley et al. 2000);

$$\widehat{K}inhom(r) = (1/A)\sum_{i}\sum_{j}\frac{1\{dij \le r\}e(xi,xj,r)}{\lambda(xi)\lambda(xj)}$$

Where A is a constant, d*ij* is a constant denominator, x*i* and x*j* are the distances between points *i* and *j* and e(x*i*,x*j*,*r*) is an edge correction factor. The edge correction is Ripley's (isotropic correction) defined as;

$$\mathrm{e}(xi,xj,r) = \frac{1}{area(\mathrm{W})\mathrm{g}(\mathrm{x}i\mathrm{x}j)}$$

Where g(x*i*x*j*) is the fraction of the circumference of the circle with center xi and radius $||xi - xj||$ which lies inside the window (W). If the hypothesis of complete spatial randomness (CSR) is rejected, then the data's tendency is towards clustering. To calculate Kinhom(*r*) in R 3.1.1 (Team 2005), the package *spatstat* is used due to its functionality in handling non uniform study areas and its use at indicating data clustering at various spatial scales.

(B)Spatial Statistics

Average Nearest Neighbour ratio & Nearest Neighbour distance

The average nearest neighbour ratio (*ANN*) measures the Euclidean distance between each feature centroid and its nearest neighbour's centroid location. It averages all these distances and provides a nearest neighbour ratio. If the ratio is less than 1, then the average distance is less than the average for the hypothetical and the point data is showing clustering patterns. If the ratio is greater than 1, then the average distance is greater than the hypothetical and the point data is showing dispersal patterns. A p-value and z-score are also computed to provide evidence of statistical significance of the patterns indicated by the nearest neighbour ratio (Clarke and Evans 1954; Cover and Hart 1967; Bailey and Jain 1978; Pinder et al. 1979; Ebdon 1980):

$$ANN = \frac{\bar{D}_O}{\bar{D}_E}$$

where *ANN* is the average nearest neighbor ratio and or a nearest neighbour distance statistic. $\bar{D}_O$ is the observed mean distance between each feature and its nearest neighbour:

$$\bar{D}_O = \frac{\sum_{i=1}^{n} d_i}{n}$$

Where $\bar{D}_E$ is the expected mean distance for the features given in a random pattern:

$$\bar{D}_E = \frac{0.5}{\sqrt{n / A}}$$

d_i equals the distance between feature *i* and its nearest neighboring feature, *n* is the total number of features, and *A* is the area of a minimum enclosing rectangle around all features, or its user-specified area value.

The nearest neighbor z-score statistic is calculated as:

$$z = \frac{\bar{D}_O - \bar{D}_E}{SE}$$

where:

$$SE = \frac{0.26136}{\sqrt{n^2 / A}}$$

To calculate NN statistic and distances in R 3.1.1 (Team 2005), the package *spatstat* and *SpatialEco* was used due to their functionality in handling inherently spatial data and their use at indicating data clustering at various spatial scales.

Getis-ord Gi statistic*

The Getis-ord Gi* statistic was used to determine significant clustering patterns of lightning-ignited wildfires within the study area per year. The Getis-ord Gi* analysis, tests spatial clustering of high and low values compared to its surrounding features; it characterizes either the high or low clustering of lightning-ignited wildfires within the study area. The G*i** statistic compares the local sum for each point *i* and its neighbors to the sum of all points, which is computed as follows (Ord and Getis 1995):

$$G_i^* = \frac{\sum_{j=1}^{n} w_{ij}x_j - \bar{X}\sum_{j=1}^{n} w_{ij}}{S\sqrt{\frac{\sum_{j=1}^{n} w_{ij}^2 + \left(\sum_{j=1}^{n} w_{ij}\right)^2}{n-1}}}$$

where *i* is the subject feature, x_j is the coordinates in space for one of the neighboring feature j, w_{ij} is the spatial weight between subject *i* and the neighboring subject *j* determine by the K nearest neighbor statistic (i.e., each feature must have 5 neighbors), $\bar{X}$ is the average distance value between all features within the study area per year, *n* is the total number of features within the study area per year, and *S* is the standard deviation of the entire study area per year given by:

$$S = \sqrt{\frac{\sum_{j=1}^{n} xij^2}{n} - (\bar{X})^2}$$

G*i** is calculated as a sum of the differences between individual values and the mean of all individuals; therefore, G*i** is a standard normal distribution z-score. G*i** produces a statistically significant result if the local sum and the expected sum are too largely different to be caused by random chance. Positive and large G*i** indicate "hotspot areas" of data clustering and low negative values indicate "cold spot areas" of data exhibiting no pattern or dispersal patterns on

the landscape. Because this statistic was based on the K nearest neighbors, we ensured during the analysis that each point possessed at least one neighbor to be considered a part of a cluster in the analysis.

Mann-Kendall Statistic

The Mann-Kendall trend statistic is a non-parametric rank correlation test between the rank observations and their time sequence which is computed as a test statistic *S* given as follows (Mann 1945; Kendall 1975):

$$S = \sum_{i=1}^{n-1} \sum_{j=i+1}^{n} aij$$

where $aij = \text{sgn}(xj - xi) = \begin{pmatrix} 1 & xi < xj \\ 0 & xi = xj \\ -1 & xi > xj \end{pmatrix}$

x_i and x_j are the rank of observations *i*th and *j*th values of the series, *n* is the length of the series. Positive value of *S* indicates an increase in trend while a negative value of *S* indicates a decrease in trend. If *S* is 0 then there is no trend detected. We applied the Mann-Kendall trend statistic to the lightning-ignited wildfire data set to test the trends in data. This statistic was employed due to its lack of requirements for data having a normal distribution (normality), as wildfire data is highly zeroed. A Pre-whitening procedure was used to account for type 1 errors. This process entailed using the nonparametric block bootstrapping and bias corrected prewhitening method and a modified Mann-Kendall test to account for type 1 errors and serial correlation in the data (Hamed 2009) using the *modifiedmk* package in R (Team 2005). The theil-sen slope was also calculated for the trend line.

In ArcGIS, a space-time cube was generated, and the emerging hotspot tool was used to identify the trends in clustering of the hexels. The space-time cube is generated by aggregated points into hexels, a count of data points that fall in each hexel per year for the entire study area and study period is calculated. The emerging hotspot analysis tool was used to display the spatial trends of the data over time. The clustering patterns of the hexels are analyzed over time by using the space time cube created as its input and conducts the Getis-Ord Gi* statistic for each hexel. The hot and cold trends detected are then evaluated by the Mann-Kendall statistic to determine whether those trends are increasing or decreasing over time. This produced a visual map in ArcGIS and is displayed in the results (Terrell and Scott 1985; Shimazaki and Shinomoto 2007; ESRI 2020).

Moran's I

Moran's I is a correlation coefficient that measures overall spatial autocorrelation of a data set based on a given set of features and its associated attributes. It then evaluates whether the pattern being exhibited by the data is clustering, dispersal or random. It calculates a Moran's I Index value, a z-score and a p-value, equation is given as follows (Moran 1950; Cliff and Ord 1981; Anselin 1995; Ord and Getis 1995);

$$I = \frac{\sum_{i\,=\,1}^{i\,=\,n} \sum_{j=1}^{j=n} wij(xi - \bar{x})(xj - \bar{x})}{\sum_{i=1}^{i=n} (xi - \bar{x})^2} - \frac{\mathrm{n}}{S_o}$$

where $S_o = \sum_{i\,=\,1}^{i\,=\,n} \sum_{j=1}^{j=n} wij$

x is the variable of interest, $\bar{x}$ is the mean of *x*, *n* is the number of spatial units indexed by *i* and *j*, wij is a matrix of spatial weights whereby convention, $wij = 0$. For a null hypothesis of no spatial autocorrelation, the expected value is;

$$E(I) = \frac{-1}{n-1}$$

Under the assumption of normality, the variance is given as;

$$Var_R(I) = \frac{\left(\left\{n\left[(n^2 - 3n + 3)S_1 - nS_2 + 3{S_o}^2\right]\right\} - \left\{k\left[(n^2 - n)S_1 - 2nS_2 + 6{S_o}^2\right]\right\}\right)}{(n-1)(n-2)(n-3){S_o}^2} - ER(I)2$$

where $S_1 = \frac{\sum_{i=1}^{i=n}\sum_{j=1}^{j=n}(wij+wji)^2}{2}$,

and $S_2 = \sum_{i=1}^{i=n}(wi.+w.i)^2$ The sum of the (ith column plus ith row) 2 of weight matrix.

$k = \frac{\left[\sum_{i=1}^{i=n}(xi-\bar{x})^4/n\right]}{\left[\sum_{i=1}^{i=n}(xi-\bar{x})^2/n\right]^2}$ This indicates the sum of each value within the matrix minus the mean.

The standard deviation and the standard z-score of I is given as;

$$SD_{R0}(I) = \sqrt{Var_{R0}(I)} \qquad z = \frac{(I - E_0(I))}{\sqrt{Var_{R0}(I)}}$$

I is given as values ranging between -1 to +1 where values near -1 indicate a negative spatial autocorrelation, values near +1 indicate positive spatial autocorrelation and values near 0 indicate no spatial autocorrelation.

To account for non-normal data, the Monte Carlo approach was used. A Monte Carlo test randomly assigns attribute values to polygons and for each permutation a Moran's I is computed.

The output is a sample distribution of Moran's I under the null hypothesis that values are randomly distributed across the entire study area. The observed Moran's I is then compared to the sampling distribution and a p-value is computed for significance. To calculate Moran's I and the Monte Carlo simulation functions in R 3.1.1 (Team 2005), the packages *spdep and sp* was used due to its functionality in handling inherently non normal and spatial data.

Chapter 3

Results

3.1 Spatial point pattern statistics

3.1.1 Getis-Ord Gi* Statistic (Hotspot Tool) in ArcGIS

All thirty-seven years of data were aggregated together and shown in *Figure 3.1*, to display one map that highlights the Getis-Ord Gi* analysis over the entire 37-year period. This was then conducted for the specific three months (June, July, and August) for all thirty-seven years and shown in *Figure 3.2, 3.3 and 3.4* respectively. The blue indicates cold clustering and red indicates hot clustering of hexels with 90% confidence over the thirty-seven-year period.

Moreover, all aggregated data points into yearly hexel layers are shown in *Figure 3.5,* and for the months of June, July, and August per year was computed into hexel layers, shown in Figure 3.6, 3.7, and 3.8 respectively, where the Getis-Ord Gi* statistic was calculated for each hexel and is displayed by the calculated z-score. A p-value and z-score of significance for clustering or dispersal patterns was computed. The orange hexels indicate positive and significant z-scores at the 90, 95 and 99% confidence intervals. The light grey hexels indicate non-significant z-score values. The blue hexels indicate significant negative z-scores at the 90,95, and 99% confidence intervals. Positive z-scores indicated significant spatial clustering of the data, where the negative z-scores signify significant dispersal patterns of the data. The prairie ecozone was excluded and is shown as white hexels.

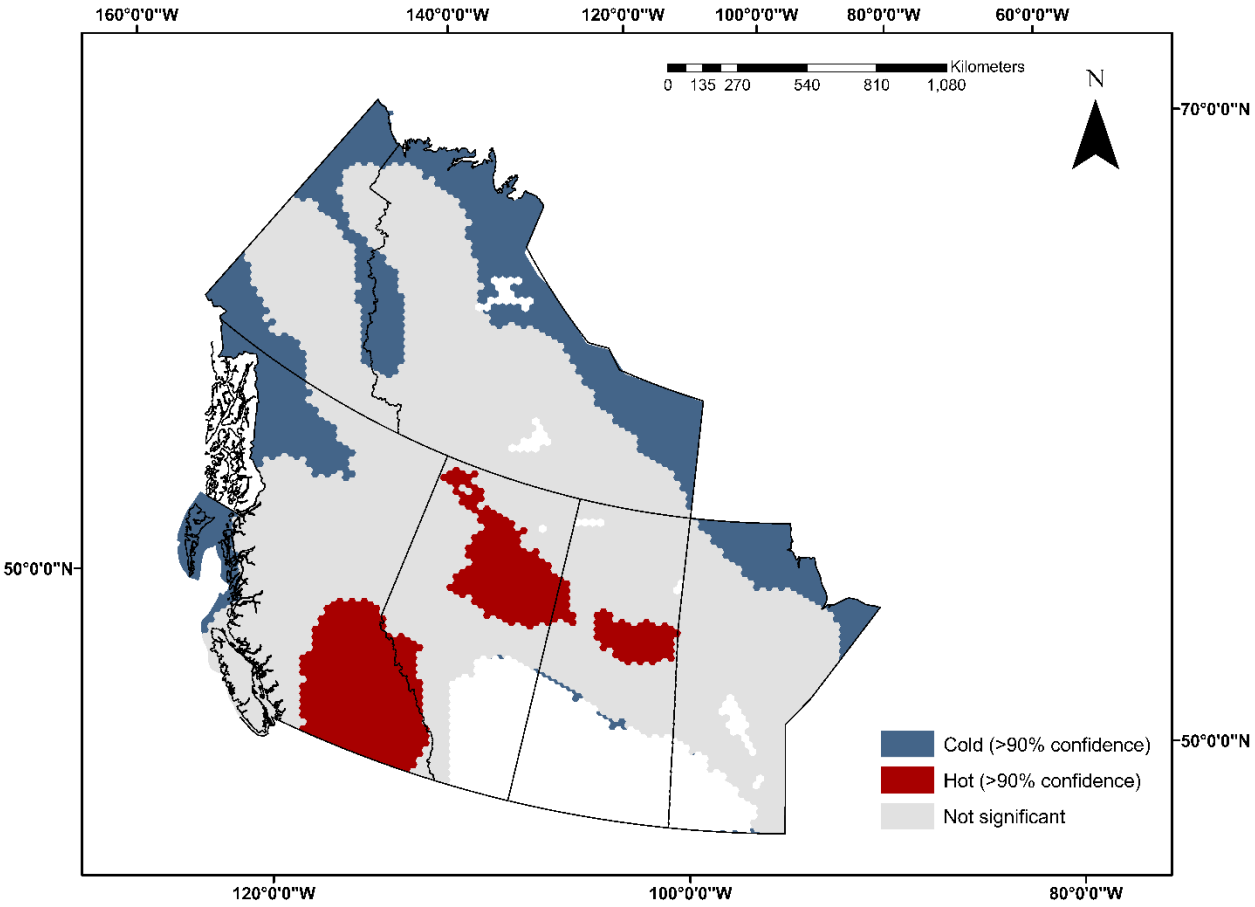

Figure 3.1: Getis-ord statistic computed for all years (1981-2018) for lightning-ignited wildfires in Western Canada. Red denotes significant (>90% confidence) clustering of hot spots, blue denotes significant (>90% confidence) clustering of cold spots and grey indicates not significant clustering.

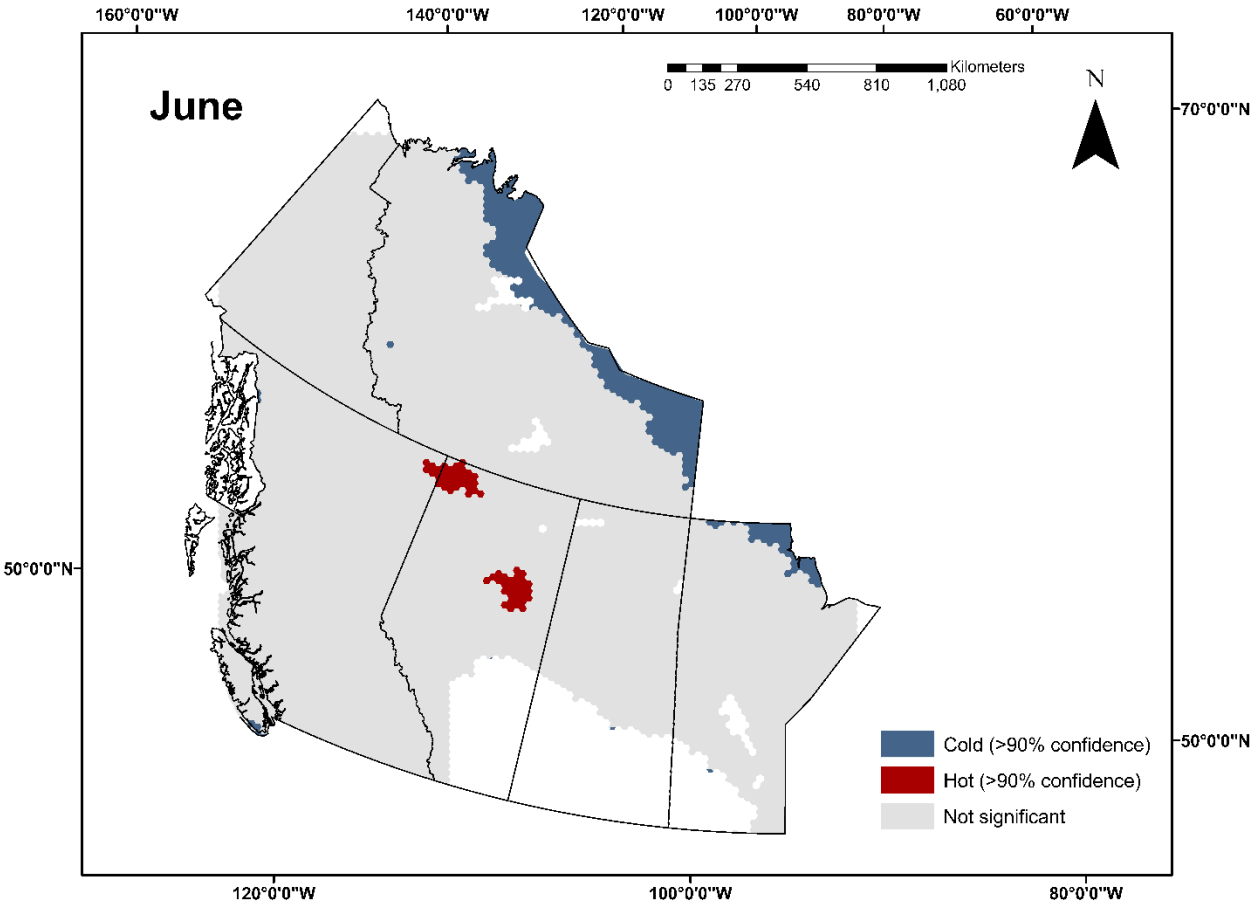

Figure 3.2: Getis-ord statistic computed for the month of June for all years (1981-2018) for lightning-ignited wildfires in Western Canada. Red denotes significant (>90% confidence) clustering of hot spots, blue denotes significant (>90% confidence) clustering of cold spots and grey indicates not significant clustering.

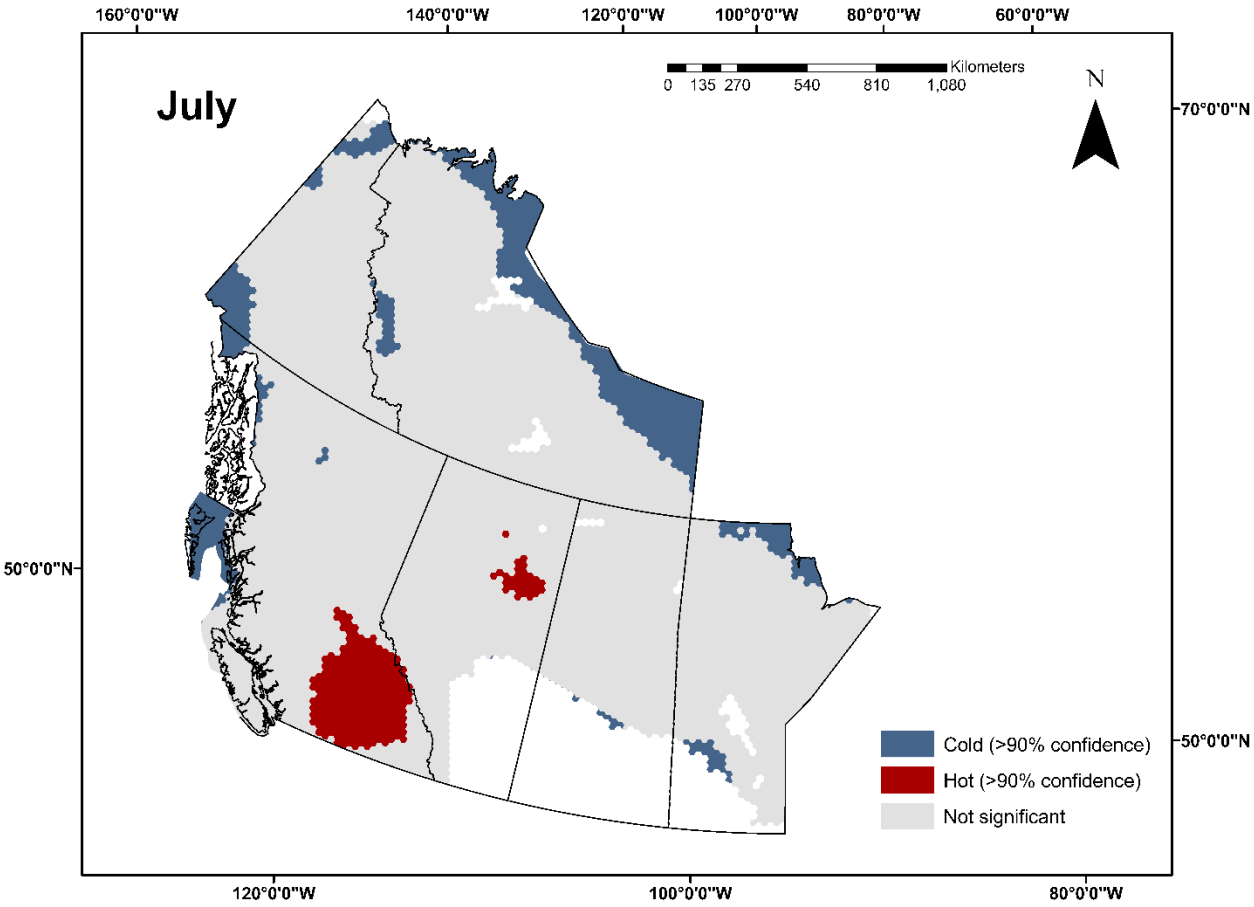

Figure 3.3: Getis-ord statistic computed for the month of July for all years (1981-2018) for lightning-ignited wildfires in Western Canada. Red denotes significant (>90% confidence) clustering of hot spots, blue denotes significant (>90% confidence) clustering of cold spots and grey indicates not significant clustering.

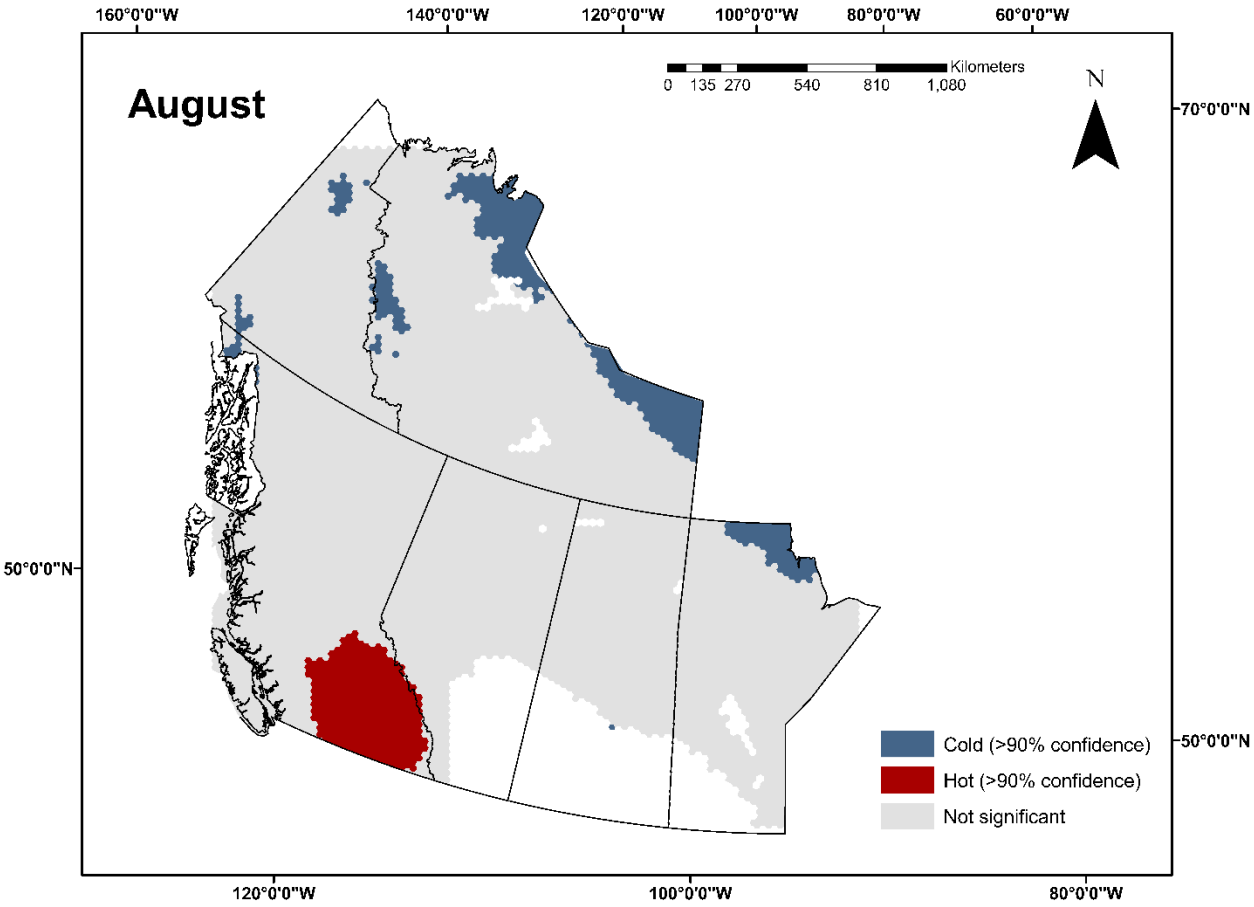

Figure 3.4: Getis-ord statistic computed for the month of August for all years (1981-2018) for lightning-ignited wildfires in Western Canada. Red denotes significant (>90% confidence) clustering of hot spots, blue denotes significant (>90% confidence) clustering of cold spots and grey indicates not significant clustering.

Figure 3.5: Getis-ord statistic computed for lightning-ignited wildfires for Western Canada by year, 1981-2018. Each graph is represented by its z-score for significance, where orange denotes significant positive z-scores at 90, 95 and 99% confidence intervals. Gray indicates no significant z-score, blue signifies significant negative z-scores at 90, 95, and 99% confidence intervals and white indicates that it was excluded from the analysis.

June

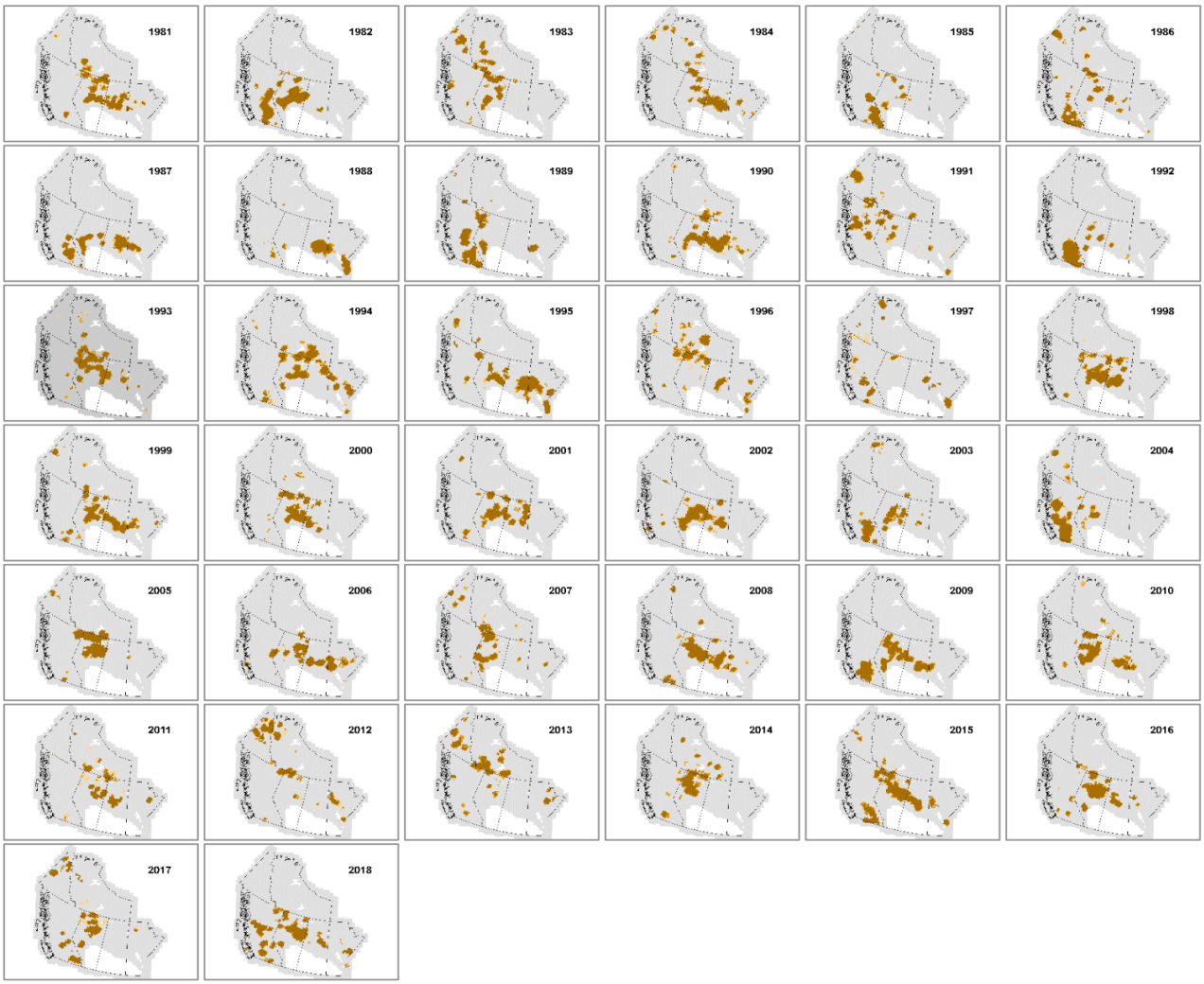

Figure 3.6: Getis-ord statistic computed for lightning-ignited wildfires in June for Western Canada by year, 1981-2018. Each graph is represented by its z-score for significance, where orange denotes significant positive z-scores at 90, 95 and 99% confidence intervals. Gray indicates no significant z-score, blue signifies significant negative z-scores at 90, 95, and 99% confidence intervals and white indicates that it was excluded from the analysis.

July

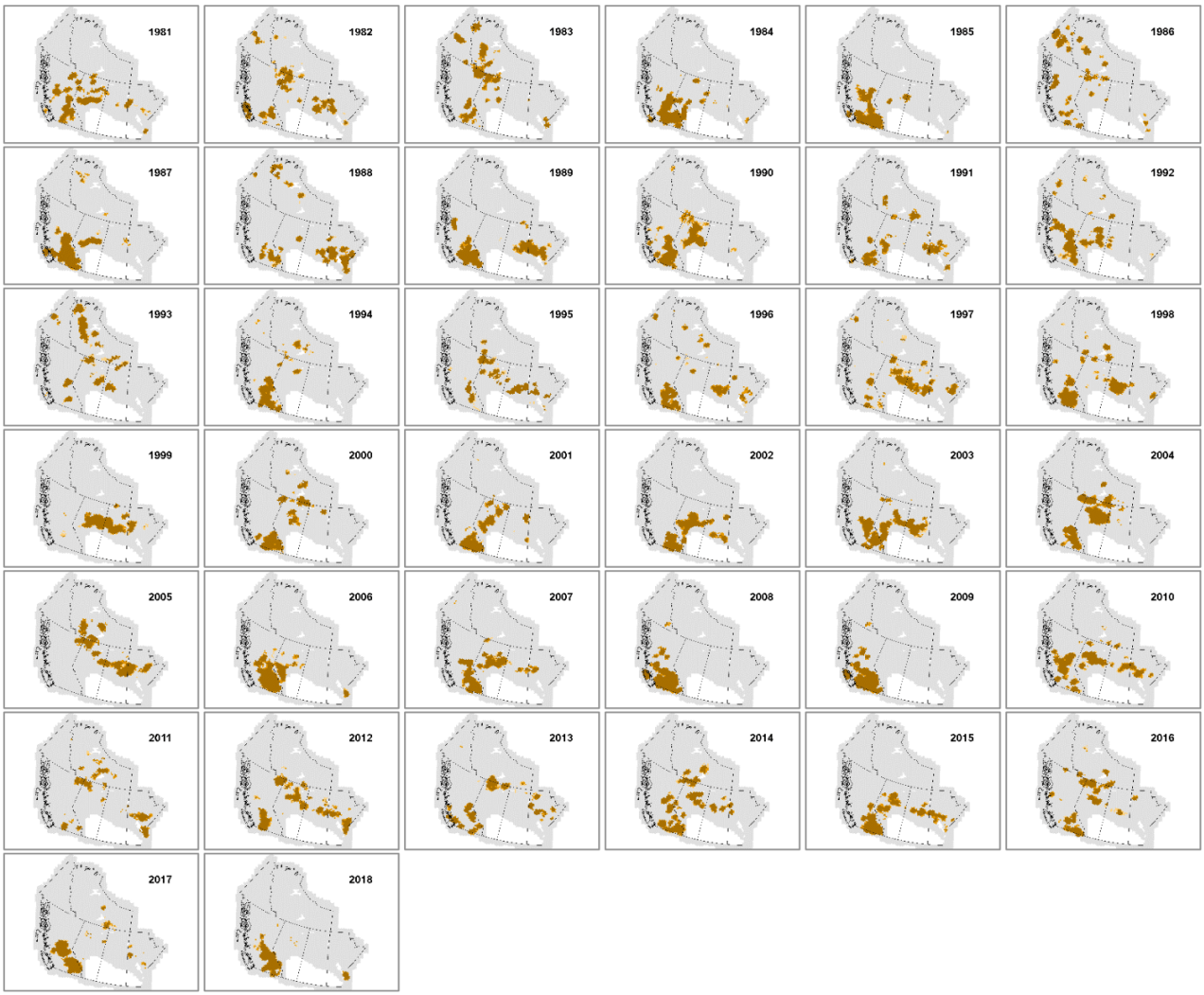

Figure 3.7: Getis-ord statistic computed for lightning-ignited wildfires in July for Western Canada by year, 1981-2018. Each graph is represented by its z-score for significance, where orange denotes significant positive z-scores at 90, 95 and 99% confidence intervals. Gray indicates no significant z-score, blue signifies significant negative z-scores at 90, 95, and 99% confidence intervals and white indicates that it was excluded from the analysis.

August

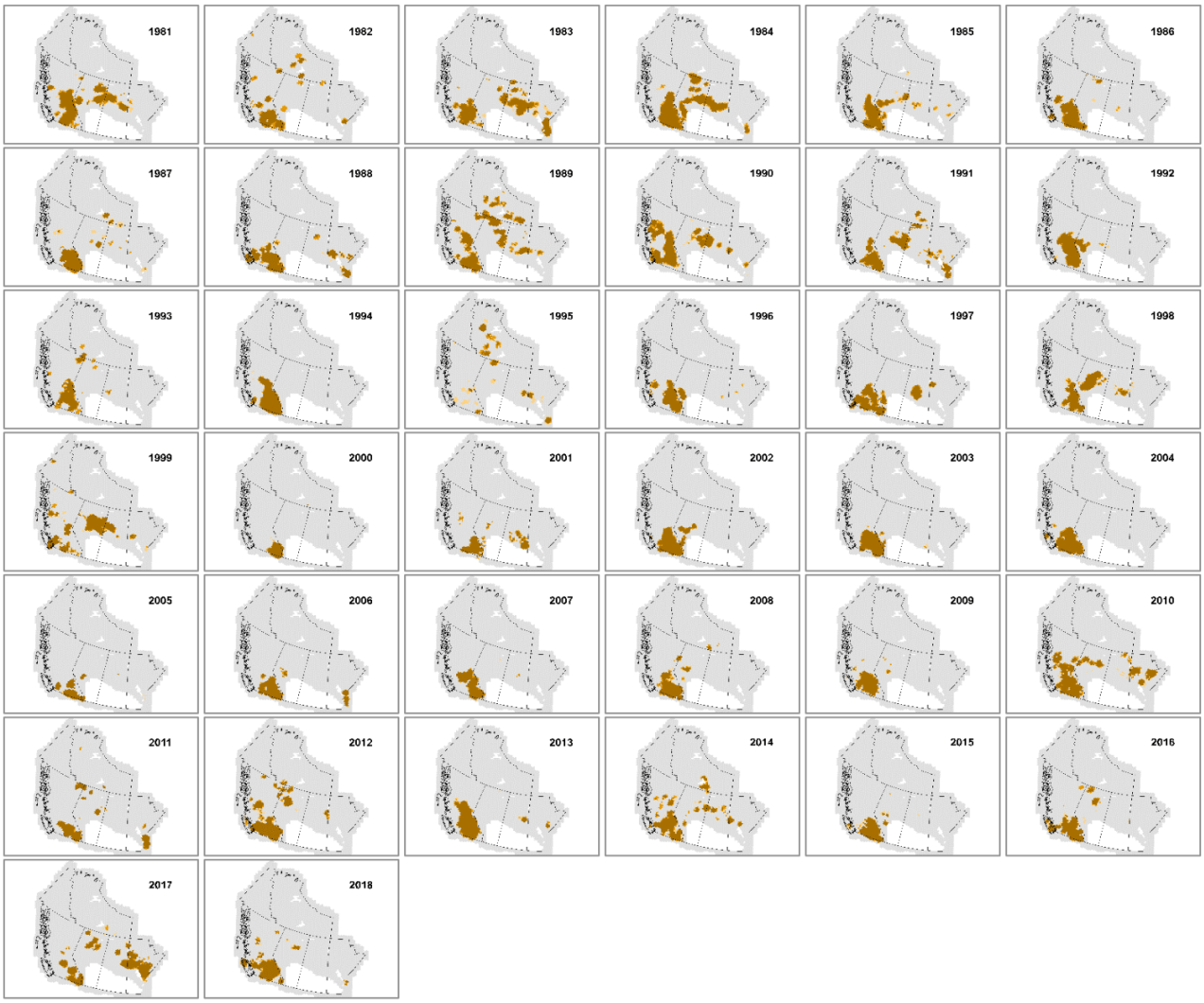

Figure 3.8: Getis-ord statistic computed for lightning-ignited wildfires in August for Western Canada by year, 1981-2018. Each graph is represented by its z-score for significance, where orange denotes significant positive z-scores at 90, 95 and 99% confidence intervals. Gray indicates no significant z-score, blue signifies significant negative z-scores at 90, 95, and 99% confidence intervals and white indicates that it was excluded from the analysis.

3.2 Temporal statistics in ArcGIS

3.2.1 Temporal Statistic (Emerging Hotspot Tool) in ArcGIS

The Mann Kendall statistic computed per hexel based on the Getis-Ord Gi* statistic for the number of lightning wildfires over the 37-year study period and study area is displayed in *Figure 3.9*. Each hexel computed a tau trend statistic, p-value and z-score to indicate if the trend was significant or not. The map is displayed by the standard deviation of the mean of each hexels z-score, where blue indicates a negative z-score and orange indicates a positive z-score. Z-scores that are <-1.8 and -1.8 to -1.5 indicate significant (negative) decreasing temporal trend scores of hexels, while >2.5, 2.2 to 2.5, 1.8 to 2.2 and 1.5 to 2.2 z-scores indicate significant (positive) increasing temporal trend scores of hexels. 1.5 to (-1.5) z-scores indicate no trend for those hexels. Therefore, these maps are detecting temporal trends in the hexels but, do not make any inferences about the spatial clustering components of the hexels and therefore do not indicate whether the increasing or decreasing hexels are hot or cold spots. Therefore, there are significant decreasing temporal hexel trends in central eastern Alberta, central eastern British Columbia, southern parts of Manitoba and Saskatchewan as well as western north and south portions of the Northwest Territories. In addition, there are significant increasing hexel trends in northern Manitoba along the Hudson Bay, northern and northwestern areas of Alberta, small pockets of the Northwest Territories around Great Slave Lake and along the south eastern edge as well as small groupings in northern Yukon and northeastern and central BC shown in *Figure 3.9*.

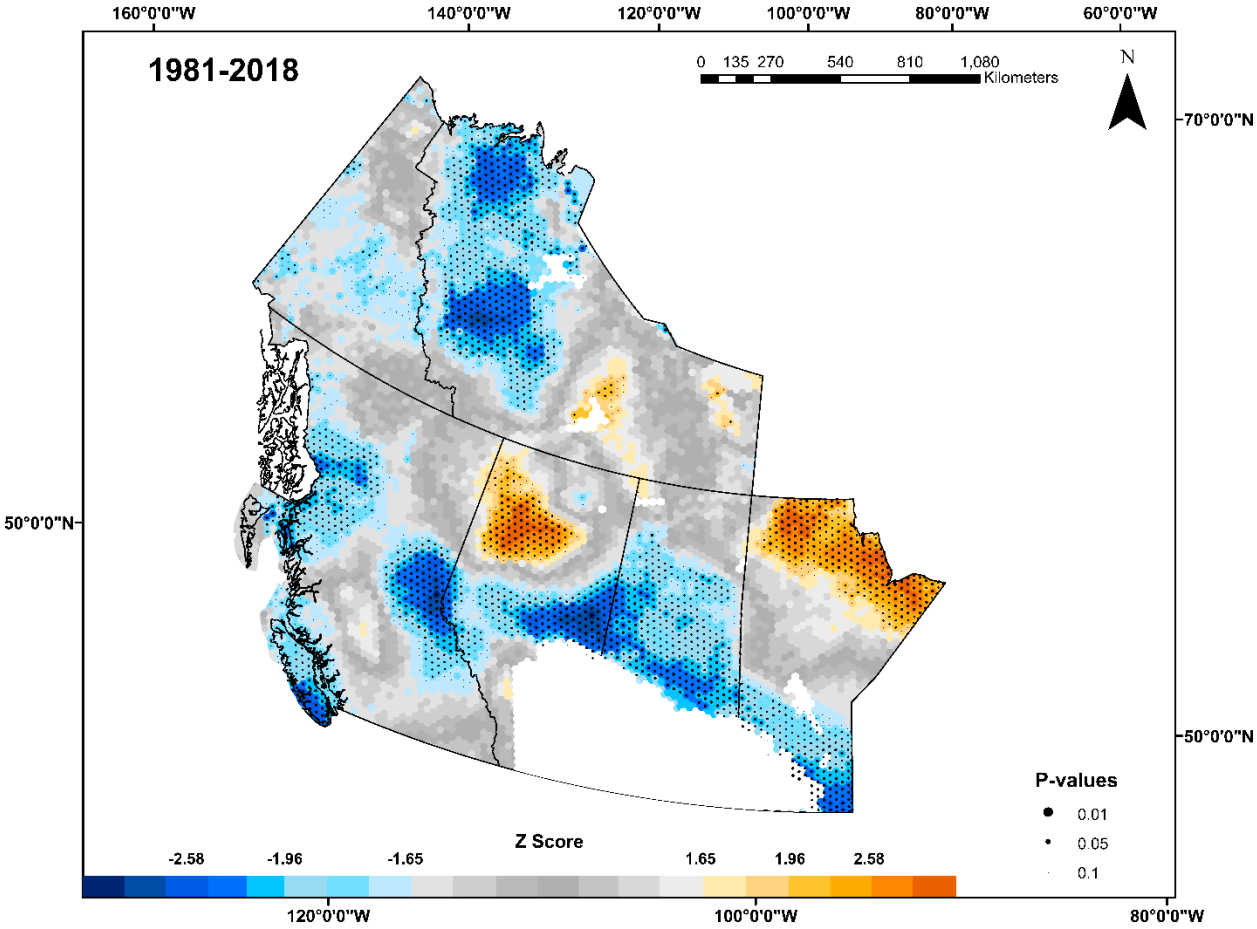

Figure 3.9: Mann-Kendall statistic computed per hexel based on the Getis-Ord Gi* z-scores for the number of lightning-ignited wildfires in Western Canada, per year, 1981-2018. Hexels are represented by the standard deviation of the z-score where orange is a positive (increasing trend) st. deviation of z and blue is a negative (decreasing trend) st. deviation of z. Dots show statistical significance based on p-values.

As for the months of June (*Figure 3.10*), July (*Figure 3.11*), and August (*Figure 3.12*) the temporal trends in hexels are displayed over the 37-year period with statistical significance indicated.

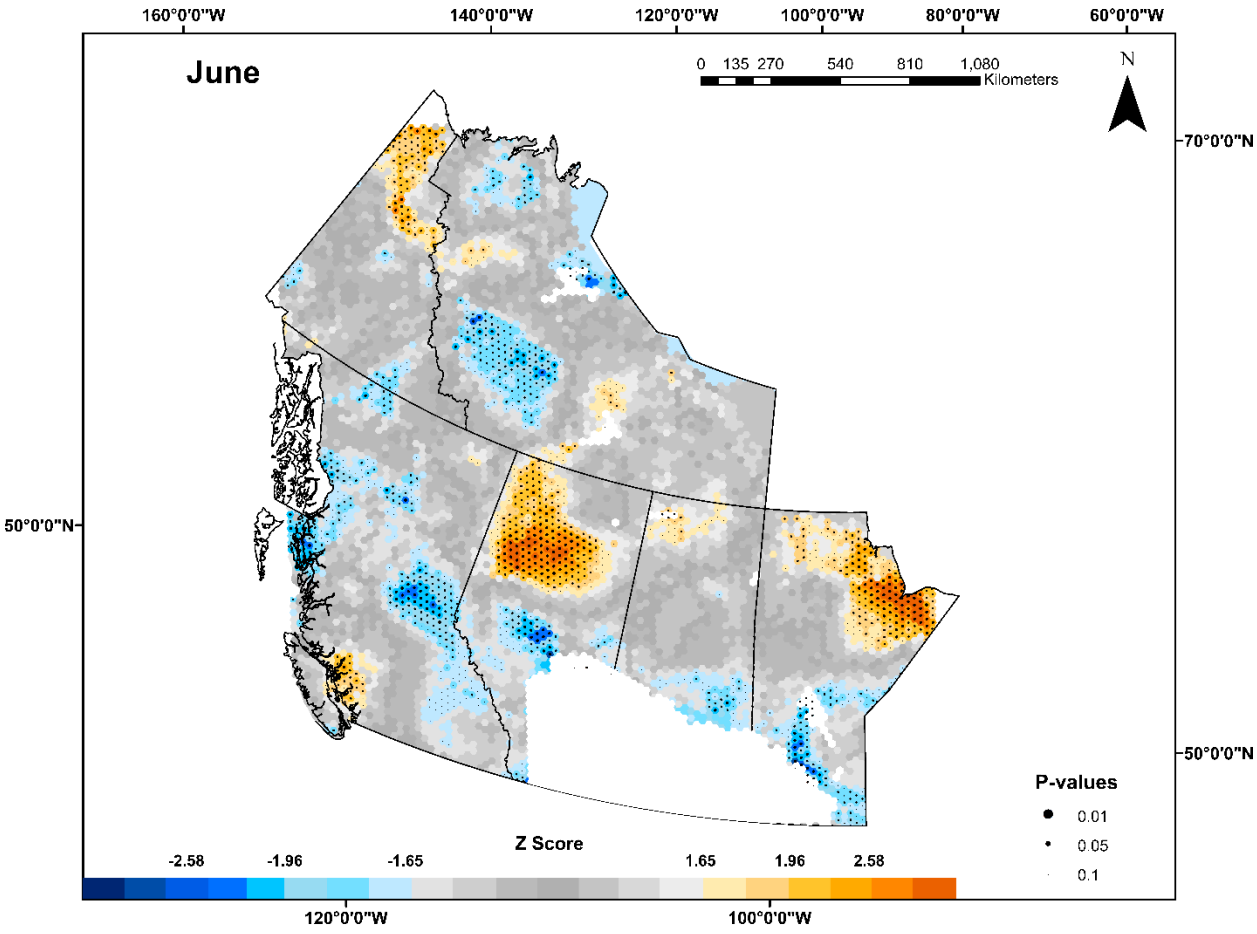

Figure 3.10: Mann-Kendall statistic computed per hexel based on the Getis-Ord Gi* z-scores for the number of lightning-ignited wildfires in June in Western Canada, per year, 1981-2018. Hexels are represented by the standard deviation of the z-score where orange is a positive (increasing trend) st. deviation of z and blue is a negative (decreasing trend) st. deviation of z. Dots show statistical significance based on p-values.

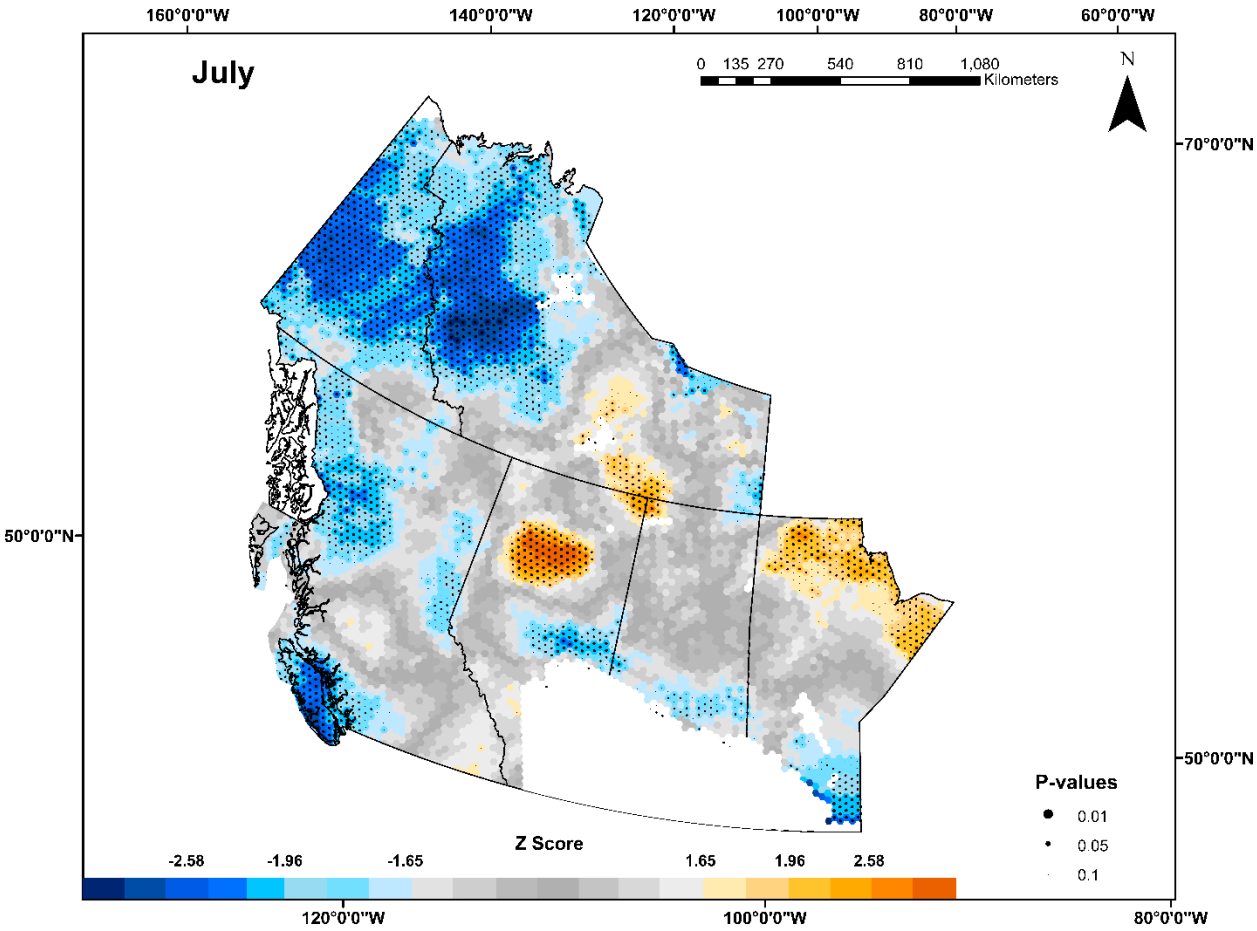

Figure 3.11: Mann-Kendall statistic computed per hexel based on the Getis-Ord Gi* z-scores for the number of lightning-ignited wildfires in July in Western Canada, per year, 1981-2018. Hexels are represented by the standard deviation of the z-score where orange is a positive (increasing trend) st. deviation of z and blue is a negative (decreasing trend) st. deviation of z. Dots show statistical significance based on p-values.

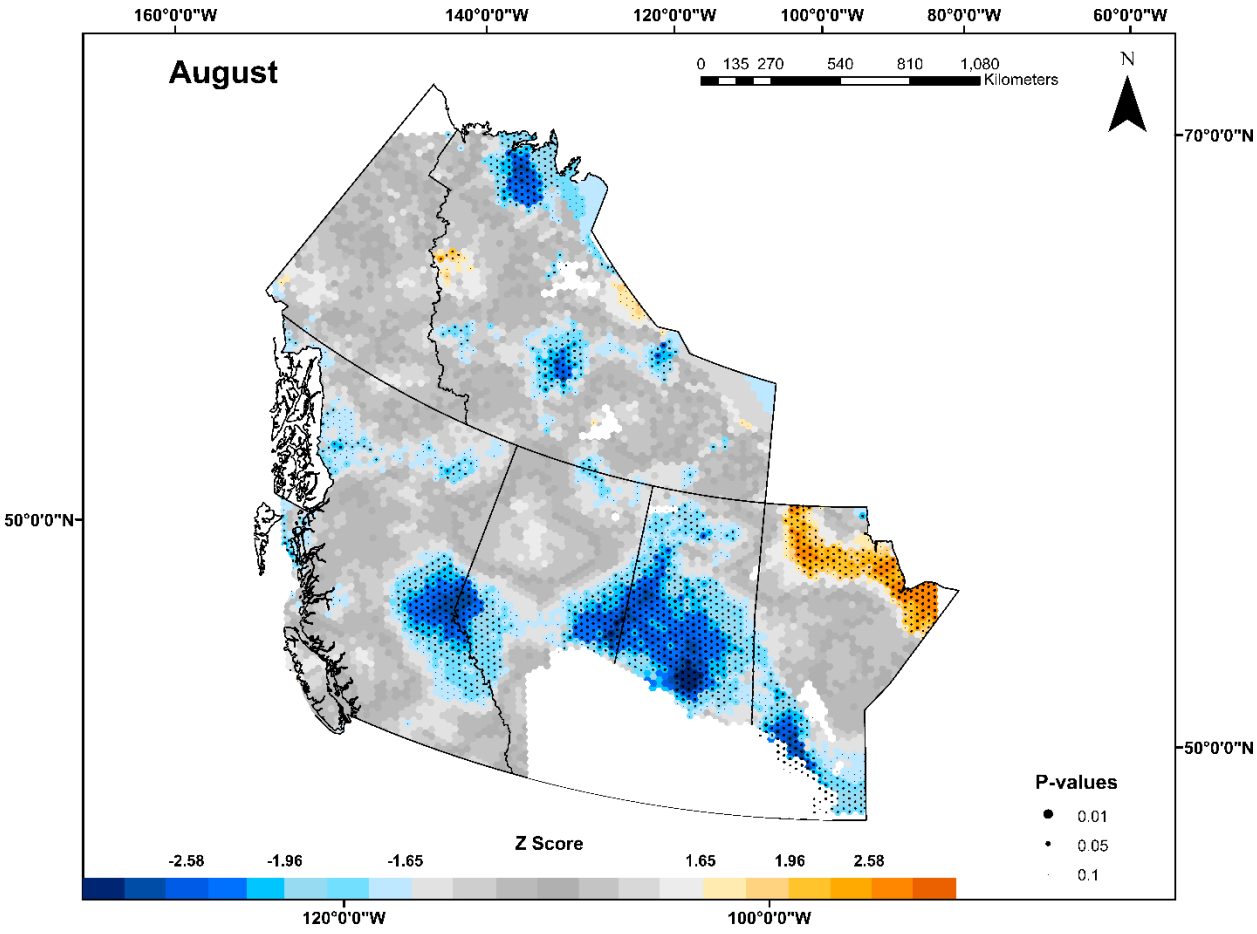

Figure 3.12: Mann-Kendall statistic computed per hexel based on the Getis-Ord Gi* z-scores for the number of lightning-ignited wildfires in August in Western Canada, per year, 1981-2018. Hexels are represented by the standard deviation of the z-score where orange is a positive (increasing trend) st. deviation of z and blue is a negative (decreasing trend) st. deviation of z. Dots show statistical significance based on p-values.

3.3 Temporal point pattern statistics

3.3.1 Temporal Statistic

The Mann Kendall statistic was computed for the entire 37-year period for the number of lightning fires with the theil-sen slope and is displayed in *Figure 3.13*. The Mann Kendall trend (tau) value for the data was -0.17, the p-value was 0.05 and the z-score computed was -1.5. Although the p-value is indicating a significance value at a confidence interval of 95%, the z-score does not and therefore the null hypothesis cannot be rejected. This indicates that there is a slight decreasing trend over the 37-year period, shown by the blue dotted line, in the data concerning the total number of lightning fires. However, it is a non-significant trend.

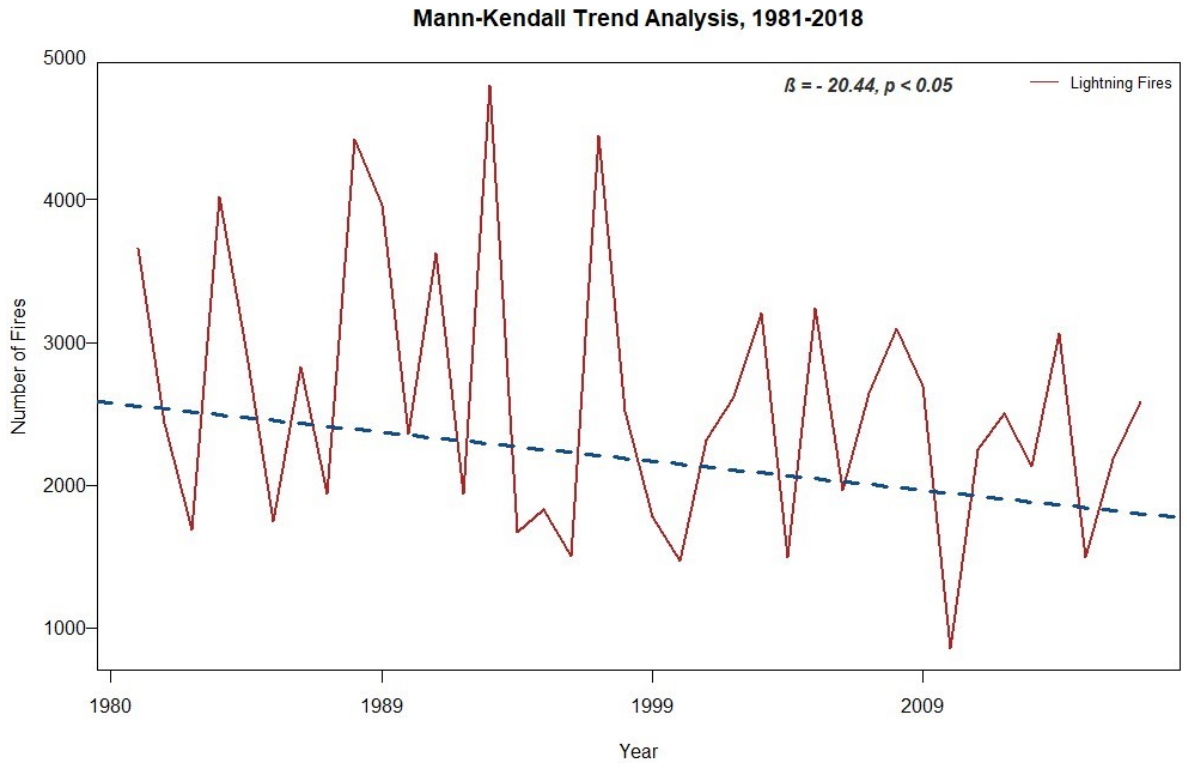

Figure 3.13: Mann-Kendall trend statistic computed for number of lightning-ignited wildfires in Western Canada between 1981-2018. The dark red line indicates the number of fires per year and the blue dotted line indicates the trend line. This statistic was computed with a theil-sen slope. The tau computed was -0.17, bootstrap p-value 0.05, z-score -1.5 and the sen slope -20.44.

The Mann Kendall statistic was computed for the months of June, July, and August for the entire 37-year period for the number of lightning fires with the theil-sen slope and is displayed in *Figure 3.14*. For the month of June, the Mann Kendall trend (tau) value for the data was -0.15, the p-value was 0.105, the z-score computed was -1.29 and the Sen slope is -5.04. This indicates that there is a non-significant decreasing trend over the 37-year period, shown by the blue dotted line, in the data concerning the total number of lightning fires. For the month of July, the Mann Kendall trend (tau) value for the data was -0.039, the p-value was 0.36, the z-score computed was -0.32 and the Sen slope is -1.69. This indicates that there is a non-significant decreasing trend over the 37-year period, shown by the blue dotted line, in the data concerning the total number of lightning fires. For the month of August, the Mann Kendall trend (tau) value for the data was -0.048, the p-value was 0.33, the z-score computed was -0.4 and the Sen slope is -3.5. This indicates that there is a non-significant decreasing trend over the 37-year period, shown by the black line, in the data concerning the total number of lightning fires. Overall, for the months of June, July, and August we found non-significant decreases in the trends for NOF's for all three months.

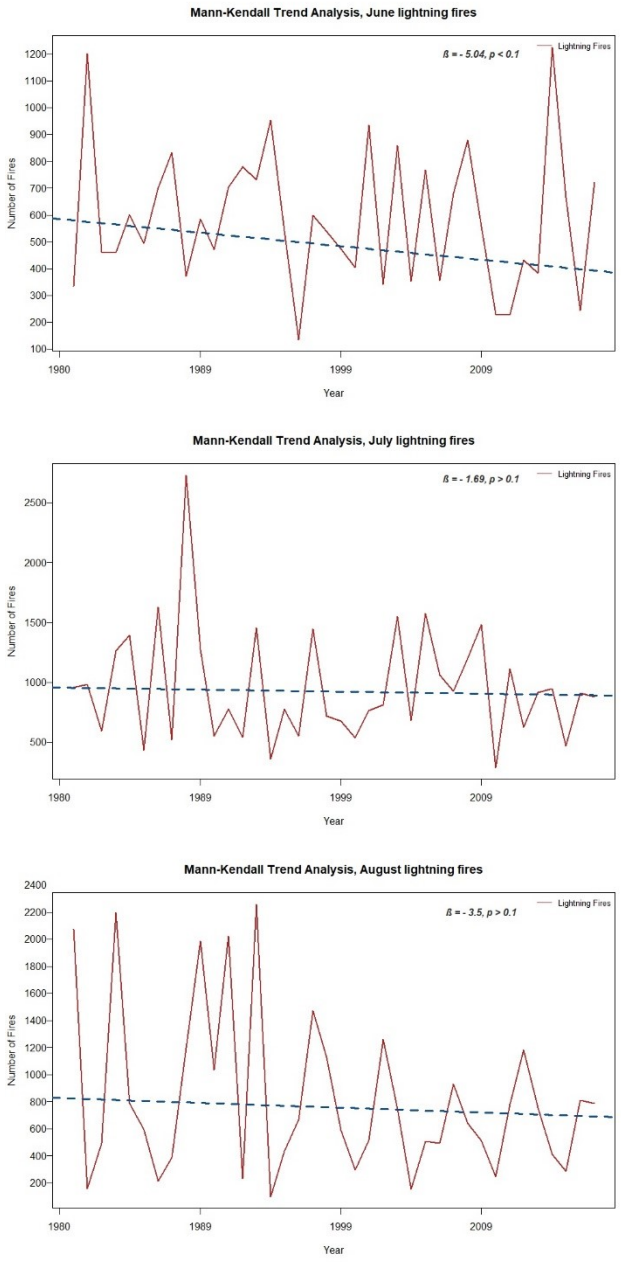

Figure 3.14: Mann-Kendall trend statistic computed for number of lightning-ignited wildfires per month (June, July, and August) in Western Canada between 1981-2018. For all months, the tau computed was between -0.15 to -0.039, bootstrap p-value was between 0.105 to 0.36, z-score was between -1.29 and -0.326 and the sen slope was between -5.0 and -1.69 for all three months.

3.4 Spatial point pattern statistics

3.4.1 Kinhom(*r*) K-function

The inhomogeneous Kinhom(*r*) K-function of a non-stationary point pattern was calculated and then graphed in *Figure 3.15*. The null hypothesis is that the data is exhibiting a spatial random point process. The black line represents the summary function of actual values from the data, while the line in red represents the expected values of a point pattern under CSR. If the black line is below the confidence bands (red line) then the spatial point pattern is deviating from the null and the data is exhibiting spatial clustering. If the black line is above the confidence bands (red line) then the spatial point pattern is deviating from the null and is showing a dispersal pattern. By determining where the red and black lines cross will indicate at what spatial scale, in kilometres, data points are clustering at, if clustering. This was computed for each analysis year (1981-2018) and shown in *Figure 3.15*. The median Kinhom(*r*) statistic for all years is 227.5 km. The highest value was 270 km in 1996 and the lowest values was 165 km in 2000 and therefore clustering is occurring between 165-270 km. All years showed a deviation from CSR indicating spatial clustering occurring within the data for each study year.

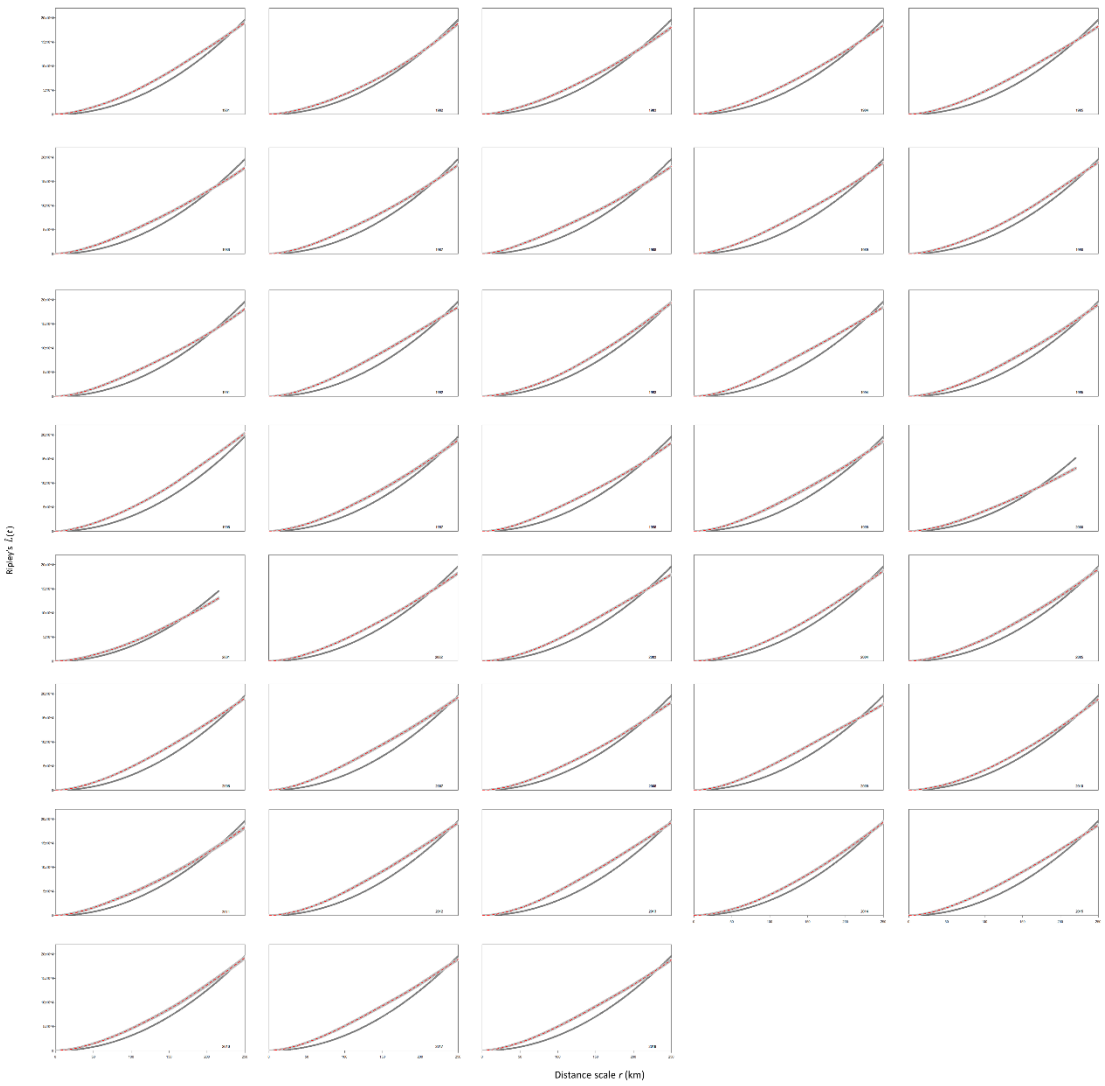

Figure 3.15: Kinhom(*r*) function for Western Canada lightning-ignited wildfires by year, 1981-2018. In each graph, the grey lines represent the upper and lower limits of the envelope based on 1000 simulations under the assumption of an independent distribution. The red line is the estimated Kinhom(*r*) function, while the black line represents the observed Kinhom(*r*) function.

3.5 Spatial statistics

3.5.1 Average Nearest Neighbour Ratio and Nearest Neighbour Statistic

The average nearest neighbour ratio (ANN) was computed and is presented in column two of Table 3.1. The associated z-score and p-value for each study year to assess significance in the spatial patterns of the data is also presented. In addition, the nearest neighbour (NN) distance statistic was calculated for each year which is seen in column three of Table 3.1. For the average nearest neighbour ratio (ANN), if ANN is greater than 1, the data is showing dispersal patterns and if the ANN is less than 1 then the data is showing clustering patterns. Confidence-intervals of 90% (+/- 1.65), 95% (+/- 1.96), and 99% (+/-2.58) were computed for the z-scores and negative z values indicate clustering patterns, while positive z-scores indicate dispersal patterns. P-values computed provided confidence intervals of 90% (0.1), 95% (0.05) and 99% (0.01). The nearest neighbour (NN) statistic calculates the distance in kilometers from one neighbour to another. The mean nearest neighbour distance per year was calculated.

All years had an average nearest neighbour ratio (ANN) under 1 (median ANN ratio was 0.474) indicating that each data year exhibited deviations from the null and thus the data points showed spatial clustering patterns. Moreover, all years had significant negative z-scores (median -48.12) indicating significant clustering of the data, coupled with significant p-values (median 0.0001). The lowest NN statistic was 104.94 km in 1994 and the highest NN statistic was 271.58 km in 2011 and therefore a range of 104-271 km of clustering was seen. The mean nearest neighbor statistic for the entire study area was 154.115 km.

Table 3.1: Average nearest neighbour ratio (<1 indicates clustering and >1 indicated dispersal**) and mean nearest neighbour (km) with associated z-score** (- is clustering and + is dispersal with confidence intervals of 90% (+/-1.65), 95%(+/-1.96), 99%(>+/-2.58**)) and p-value (**confidence intervals of 90%(<0.1), 95%(<0.05), and 99%(<0.01)**) was computed for lightning-ignited wildfires in Western Canada, by year, 1981-2018.**

Year	NN Ratio	Mean NN (km)	Z-Score	P-value
1981	0.45	110.87	-63.57^{+}	0.0001*
1982	0.496	156.71	-47.523^{+}	0.0001*
1983	0.51	189.85	-38.75^{+}	0.0001*
1984	0.46	112.15	-65.46^{+}	0.0001*
1985	0.43	118.09	-59.11^{+}	0.0001*
1986	0.489	180.24	-40.7^{+}	0.0001*
1987	0.47	131.52	-53.49^{+}	0.0001*
1988	0.455	151.88	-45.9^{+}	0.0001*
1989	0.49	115.83	-63.7^{+}	0.0001*
1990	0.46	115.46	-65^{+}	0.0001*
1991	0.508	164.2	-45.6^{+}	0.0001*
1992	0.43	113.01	-65.4^{+}	0.0001*
1993	0.478	175.14	-43.9^{+}	0.0001*
1994	0.46	104.94	-71.2^{+}	0.0001*
1995	0.5	186.75	-38.7^{+}	0.0001*
1996	0.5	184.82	-40.5^{+}	0.0001*
1997	0.45	188.89	-40.1^{+}	0.0001*
1998	0.45	107.41	-69.3^{+}	0.0001*
1999	0.47	147.12	-49.9^{+}	0.0001*
2000	0.48	159.32	-41.4^{+}	0.0001*
2001	0.51	179.52	-36^{+}	0.0001*
2002	0.43	130.16	-52.33^{+}	0.0001*
2003	0.44	124.39	-54.5^{+}	0.0001*
2004	0.511	127.31	-52.9^{+}	0.0001*
2005	0.52	198.66	-35^{+}	0.0001*
2006	0.44	159.32	-61.1^{+}	0.0001*
2007	0.46	165.77	-45^{+}	0.0001*
2008	0.448	135.38	-54.3^{+}	0.0001*
2009	0.42	109.25	-61.4^{+}	0.0001*
2010	0.47	145.32	-51.8^{+}	0.0001*
2011	0.51	271.58	-26.9^{+}	0.0001*
2012	0.533	172.54	-42.4^{+}	0.0001*
2013	0.515	156.35	-46.4^{+}	0.0001*
2014	0.52	165.88	-42.8^{+}	0.0001*
2015	0.5	137.08	-52.66^{+}	0.0001*
2016	0.49	208.95	-37.2^{+}	0.0001*
2017	0.49	166.78	-45.1^{+}	0.0001*
2018	0.46	141.79	-52.9^{+}	0.0001*

*Significant P-value $^{+}$ Significant Z-score

3.5.2 Moran's I Tool of spatial autocorrelation

Moran's I statistic of spatial autocorrelation was computed for the data set where the null hypothesis is that the spatial process being exhibited by the data is by random chance. The Moran's I statistic needs to be evaluated along with its p-value and z-score for significance. The results are shown in Table 3.2. The median value for Moran I is 0.85 with a median p-value of 0.00167 and a median z-value of 117, indicating that the data for the entire study period (1981-2018) exhibits some form of spatial autocorrelation and spatial clustering of like values. The Moran I values were between 0.91 and 0.72. The z-score ranges were between 98 and 124, with the highest z-score in 1994 and 2009 and the lowest in 2018. All p-values for each year showed a significant value of 99% confidence interval (<0.01) and all z-scores for each study year showed a significant value of 99% confidence interval (>2.58).

Table 3.2: Moran I's correlation coefficient of spatial autocorrelation with the Monte Carlo simulation for lightning-ignited wildfires in Western Canada, per year, 1981-2018. A p-value and z-score were also computed for significance, where z-score (+ is clustering and - is dispersal with confidence intervals of 90% (+/-1.65), 95%(+/-1.96), 99%(>+/-2.58)**) and p-value (**confidence intervals of 90%(<0.1), 95%(<0.05), and 99%(<0.01)).

Year	Moran I	P-value	Z-score
1981	0.86	0.00167*	118+
1982	0.82	0.00166*	112+
1983	0.77	0.00166*	105+
1984	0.88	0.00167*	120+
1985	0.88	0.00167*	120+
1986	0.83	0.00166*	114+
1987	0.86	0.00167*	118+
1988	0.85	0.00166*	116+
1989	0.87	0.00167*	119+
1990	0.86	0.00166*	117+
1991	0.81	0.00166*	111+
1992	0.9	0.00167*	123+
1993	0.77	0.00166*	105+
1994	0.9	0.00167*	124+
1995	0.79	0.00166*	107+
1996	0.78	0.00166*	107+
1997	0.79	0.00166*	108+
1998	0.89	0.00167*	121+
1999	0.87	0.00167*	118+
2000	0.85	0.00166*	117+
2001	0.83	0.00166*	113+
2002	0.85	0.00166*	117+
2003	0.89	0.00167*	122+
2004	0.86	0.00166*	118+
2005	0.79	0.00166*	107+
2006	0.87	0.00167*	119+
2007	0.85	0.00166*	116+
2008	0.87	0.00167*	119+
2009	0.91	0.00167*	124+
2010	0.83	0.00166*	114+
2011	0.72	0.00166*	98+
2012	0.81	0.00166*	110+
2013	0.86	0.00166*	117+
2014	0.80	0.00166*	110+
2015	0.87	0.00167*	119+
2016	0.80	0.00166*	110+
2017	0.82	0.00166*	112+
2018	0.86	0.00166*	117+

*Significant P-value +Significant Z-score

Chapter 4

Discussion

4.1 Overview

Determining trends and spatial characteristics of lightning fires is a challenge as records are incomplete across Canada. Significant efforts from multiple researchers has led to a more comprehensive look and standardized dataset which is being used to conduct research on wildfires in Canada. The idea of lightning-caused wildfires clustering over space and time is not a new concept, however, few studies have used ArcGIS to quantify these spatial-temporal patterns. Using ArcGIS to analyze this data was a challenging process. However, using this spatial program to visualize the data is a valuable tool in presenting research and can broaden the understanding of statistics to multiple audiences. Moreover, few studies have considered analyzing the entire Canadian National fire database, as most studies that used this database excluded points from the analysis based on the size of the area burnt per fire. Although there are inherent data quality issues (incomplete and missing records), looking at all fires, no matter what size of area they burned, is extremely valuable in understanding the natural processes of lightning-caused wildfires as well as how climate change is affecting these interactions. Furthermore, the dataset was quite large (97,921 data points) indicating that results from this analysis could be considered representative of the population being analyzed.

For Kinhom(r) K-function, we found that the data was exhibiting spatial clustering from 165 km to 270 km and for the NN statistic we found clustering from 104 km to 271 km for lightning-ignited fires in Western Canada from 1981-2018. These results are like other studies who have looked at spatial patterns and found similar results of clustering, examples include, 2km and up in Florida, USA (Genton et al. 2006), up to 200 km in Alberta (Wang and Anderson

2010) and approximately 200 km in Ontario (Podur et al. 2003). Even though this research looked at a broader study area than previous studies, similar results were seen.

We found significant hotspot clustering occurring each year of the study for lightning-ignited wildfires. Specifically, over the 37-year period we can see that hexels containing hot spot clustering occurred in Northern Alberta, Saskatchewan, and South eastern British Columbia. This spatial clustering pattern of lightning fires is similar to other studies such as Podur et al. (2003); Genton et al. (2006); Wang and Anderson (2010); Masrur et al. (2018) in terms of the spatial distribution on the landscape. However, these studies used kernel density estimations to spatially display their lightning patterns and this research used the Getis-ord Gi* statistic. Both statistics are slightly different, where kernel density tests and displays the intensity of the point pattern at certain locations, and the Getis-ord Gi* statistic measures spatial association in the data. However, they both test the data's spatial distribution patterns, and similar spatially significant areas on the landscape were found between this research and the four mentioned.

We found that for Moran's I spatial autocorrelation statistic for all years (1981-2018) lightning-ignited wildfire intensities are significantly spatially autocorrelated. These results are similar to Masrur et al. (2018) who found that wildfires in the circumpolar tundra from 2001 to 2015 showed significant spatial autocorrelation.

We found that for the entire study area, the NOF showed an overall non-significant decreasing trend over time. This is similar to Hanes et al. (2019) who found a non-significant decreasing trend in the data for NOF nationally since 1959, found in their Figure 3 b). Moreover, Coogan et al. (2018) saw an overall decrease in NOF over Canada from the same time period, 1981-2018. Campos-Ruiz et al (2018) found a non-significant decreasing trend for NOF caused

by lightning, but also observed that NOF by lightning showed strong oscillation peaks every ~ 12 years in Wood Buffalo National Park, Alberta. Although these results are similar, a step further was taken in this analysis by using ArcGIS to map the trends per hexels over space and time. This resulted in a visual representation of each hexel *(Figure 3.9*) showing where it was significant, non-significant, increasing, decreasing and no trend from 1981-2018. These maps along side the Getis-Ord Gi* maps can indicate if the increasing or decreasing trend hexels are hot or cold spots. This provided a detailed analysis for trends and indicated variability on the landscape. Hanes et al (2019) produce a similar spatial visual map showing NOF (>200 ha) in Canada delineated by homogeneous fire-regime zones and the associated trend. Although their study only looked at fires over 200 ha, similar geographical areas were found between their study and this one. For hot and cold spot clustering, it was found that for the entire study area and period, Northern Alberta, Saskatchewan, and British Columbia experiences temporal hot spot clustering, while Northern Manitoba experiences cold spot clustering. In conjunction, it can be assessed that the hot spot clustering in Alberta is increasing in its temporal trend, the hot spot clustering in Saskatchewan is decreasing in its temporal trend, the cold clustering in Northern Manitoba is increasing in its temporal trend and for British Columbia's hot spot clustering there is not trend detected. As for the seasonality component, it can be seen that Northern Alberta is experiencing an increase in temporal hot spot clustering hexel trends for the months of June and July, while British Columbia is experiencing hot spot clustering for the 37-year period for both the months of July and August. These areas could be of major concern for fire managers and more information and research is needed to determine the extent of the increase in fire activity over this period.

A thing to note about the Northern Areas (Northern Alberta, Manitoba and the Northwest Territories) is that since these places cover large areas with minimal population and with increases in technology and awareness of wildfires records, these results could be showing increases in trends in these areas due to an increase in reporting and more resources available. Therefore, these areas should be researched further as, if the case concerning NOF are increasing then investigating the cause of these increases are valuable in determining how climate change is changing these vulnerable areas and what these landscapes could experience in the future. This is important as northern regions are facing extensive changes to their ecosystems due to climate change (Turetsky et al. 2017). Examples include spruce dominated forests in Alaska becoming vulnerable due to more frequent fire-return intervals and late season burning (Kasischke et al. 2010), northern treelines are moving into previous occupied tundra ecosystems (Weber and Flannigan 1997), increased in frequency of extreme fire weather in Canada is projected for northern fire zones (Wang et al. 2015), warming in the north could create a risk of permafrost thaw (Schuur et al. 2013) and areas burned by severe wildfires will affect the resilience of permafrost and could lead to vegetation changes where grasslands and or deciduous dominated forests could be favoured (Chapin et al. 2010).

The results of this study suggest that lightning fires are variable over space and time but show significant spatial clustering patterns on the landscape over time in certain areas within Western Canada. This clustering could be due to large-scale climatic patterns (Gedalof et al. 2005) such as El Nino (Fauria and Johnson 2006), mesoscale circulations (Dissing and Verbyla 2003), fuel moisture (Larjavaara et al. 2005), anthropogenic factors (Parisien et al. 2006), drought (Meyn et al. 2010), diurnal heating and cooling cycle (Burrows and Kochtubajda 2010), type of tree cover (Krawchuk et al. 2006; Veraverbeke et al. 2017), localized thunderstorm

activity (Liu and Li 2016), associated temperature, precipitation present (Mundo et al. 2013; Whitman et al. 2015), and increased lightning densities and distributions (Wierzchowski et al. 2002; Romps et al. 2014). Further research looking into a broad scaled study on what is causing these recurring spatial and temporal patterns and why it is being cause could provide a huge amount of details into understanding the processes of why lightning fires initiate in certain areas, what drivers are causing changes in theses patterns, and how this will look in a changing climate.

In terms of this research study, it can be speculated that various factors are contributing to the spatial and temporal clustering patterns observed, although further investigative research is needed to fully understand the factors playing a role in these spatial patters. For spatial distribution patterns, Veraverbeke et al (2017) found that for Alaska and the Northwest territories, climate (temperature, precipitation and convective precipitation) and vegetation cover accounted for 56% of the variability seen in lightning strike densities, while 48% was attributed to climate alone. Vázquez and Moreno (1993) found that temperature and precipitation were the best predictors of total area burned and NOF within their study in Spain. Van Wagtendonk and Cayan (2010) found that bioregions were an excellent indicator in distinguishing differences in spatial patterns of lightning within their study in Yosemite, US. Masrur et al (2018) found a significant association between climate conditions and NOF in Alaska and Northwest Territories, as well as an increase in NOF associated with a decrease in soil moisture level, precipitation and an increase in surface temperatures. Campos-Ruiz et al (2018) also found that mean annual temperature and relative humidity was correlated to lightning-caused fires in Wood Buffalo National Park, Alberta. Therefore, potential variables driving spatial distributions of lightning fires on the western Canadian landscape are climate (temperature and precipitation) as well as

vegetation type. However, further research needs to be undertaken to determine the exact variables affecting the spatial distribution patterns for this landscape.

As for temporal clustering, major land-water boundaries (Orville et al. 2002), elevation (Reap 1991; Van Wagtendonk and David 2009), topography (Dissing and Verbyla 2003), and elevated terrain features (Orville et al. 2002) all play a role in wildfire initiation. Masrur et al (2018) found that most of their wildfire events occurred in June, July and August. Podur et al (2003) suggested elevation and local elevated terrain features play a role in ignition probability in Ontario, Canada. Van Wagtendonk and Cayan (2010) also found elevation had a direct effect in lightning distributions, where lightning strike densities occurred at high rates in mountain and desert regions. Kilinc and Beringer (2007) found that vegetation and elevation played a role in lightning density, where differential heating associated with vegetation cover resulted in mesoscale circulation patterns that create and influence lightning strikes. Moreover, Larjavaara et al (2005) observed north-south gradients for lighting fires in their study area of Finland over time and attribute this to latitude/longitude. In terms of this research study, it can be speculated that for the temporal distribution patterns, large scale climatic patterns, local terrain features, topography and forest cover play a role in the temporal distributions within the study area.

Climate and forest coverage are the biggest variables in determining the spatial and temporal patterns of lightning fires. However, they are highly influenced by various factors that are theorized to be exacerbated and shift with climate change (Wotton and Flannigan 1993; Weber and Stocks 1998; Stocks, et al. 2000). It is predicted that with anthropogenic climate change, warmer and drier environments will be experienced (Weber and Flannigan 1997; Weber and Stocks 1998; Stocks, et al. 2000), drier fuels will occur on the landscape (Flannigan et al. 2016; Wotton et al. 2017) and lightning densities with increase (Romps et al. 2014; Blouin et al.

2016; Veraverbeke et al. 2017) leading to longer fire seasons (Wotton and Flannigan 1993; Jain et al. 2017; Hanes et al. 2019), more larger mega wildfires on the landscape (Kasischke et al. 2010) which will affect the human expansion into forest areas increasing the WUI (Wang and Anderson 2010; Robinne et al. 2016; Campos-Ruiz et al. 2018; Johnston and Flannigan 2018). Further research needs to be conducted on how these spatial and temporal patterns will be affected in a changing climate as this could have serious implications for forest health, communities, and fire managers.

4.2 Limitations

Like multiple long-term national dataset studies data quality is an issue, notably with respect to incomplete datasets and mapping accuracy (Stocks et al. 2003; Robinne et al. 2016; Coogan et al. 2018; Hanes et al. 2019). A shortcoming of this study is the fact that we considered all wildfires, even small fires (< 200ha). These fires are considerably unreliable for NOF as they are severely underreported due to inconsistencies within differing fire management agencies (Bridge et al. 2005; Magnussen and Taylor 2012). However, fires below <200 ha account for ~97% of wildfires (Stocks et al. 2003) and are therefore valuable when determining lightning-initiated wildfires and how they are clustering on a landscape over space and time. Moreover, they are a huge part to play as they have the potential to provide important information to wildfire research (Coogan et al. 2018; Hanes et al. 2019). Therefore, it was deemed that valuable information could still be obtained by looking at the entire data set without subsetting by area burned due to the amount of data points available and the objective of gaining further insight into spatial and temporal patterns of lightning-caused wildfires.

Other limitations of the data include the distinction between lightning and human-cause fires. This distinction is highly variable as it is decided by workers on the ground and therefore the accuracy relies on their knowledge. Furthermore, fire management and policies drive this distinction as well and since these regulations change over time, looking at large time scaled datasets are difficult to decipher for accuracy (Robinne et al. 2016; Campos-Ruiz et al. 2018; Coogan et al. 2018; Hanes et al. 2019). There have been significant upgrades in the dataset since 1980 to increase its reliability. The results concur with other research that have attempted to navigate these data quality issues (Podur et al. 2003; Wang and Anderson 2010; Masrur et al. 2018; Coogan et al. 2018; Hanes et al. 2019), giving confidence that the spatial and temporal clustering patterns of lightning-initiation wildfires in Western Canada are representative.

Another caveat to consider is that this study did not consider human-caused wildfires which have been of major concern within recent years, due to their destructive capacity and effects on the landscape. Although various studies compare the two types of wildfire causes such as Wang and Anderson (2010); Campos-Ruiz et al (2018); Coogan et al (2018); Hanes et al (2019), this was not considered in the study due to the focus on lightning and its effects on the Canadian landscape and how it is changing with anthropogenic climate change (Flannigan and Wotton 1991; Wotton et al. 2010; Romps et al. 2014).

Lastly, we did not consider area burned in this study. This is a major factor when considering the effects of wildfires on the landscape, forest mosaics, reburn, changes in forest composition, pyro cumulous clouds and how wildfires spread (Whitman et al. 2015; Jain et al. 2017; Hanes et al. 2019; Rodrigues et al. 2019). Also, fires based on area burned are more accurately reported and are therefore considered more reliable when conducting research (Podur et al. 2003; Hanes et al. 2019). Although areas burned on the landscape play a factor in wildfire

initiations, this aspect was not considered and therefore could be an area of further study to quantify how burned area affect the processes underlining spatial and temporal patterns of lightning strikes and densities which result into wildfires.

Chapter 5

Conclusion

5.1

This study has illustrated that lightning-caused wildfires vary over a broader spatial and temporal scale in Western Canada from 1981-2018. We found evidence to support that lightning fires are spatially clustering between 104 - 270 km. Moreover, we found that over the thirty-seven-year period, Northern Alberta, parts of Saskatchewan and British Columbia experienced consistent hot spot clustering of lightning-ignited wildfires. Specifically, Northern Alberta saw an increase in the trend of hot spot clustering. August and July saw hot spot clustering of lightning fires in British Columbia, while June and July saw an increasing trend in hot spot clustering in Northern Alberta. Overall, there is a non-significant decreasing trend for the total NOF as well as for the months of June, July, and August. Further research is needed to answer questions about what variables are contributing to this clustering and how this clustering will be affected by climate change. As a broad scale study, looking at broad scale factors such as global weather phenomena's (i.e. El Nino), forest cover and topography could provide interesting information on reasons behind lightning fire occurrences. This is especially relevant and important as lightning densities are projected to increase (Romps et al. 2014; Veraverbeke et al. 2017) and move further north, into regions where wildfires have the capacity to be destructive for ecosystems and communities (Turetsky et al. 2015; Masrur et al. 2018).

References

Anselin L. 1995. Local Indicators of Spatial Association—LISA. Geogr Anal. 27(2):93–115. doi:10.1111/j.1538-4632.1995.tb00338.x.

Baddeley AJ, Møller J, Waagepetersen R. 2000. Non- and semi-parametric estimation of interaction in inhomogeneous point patterns. Stat Neerl. 54(3):329–350. doi:10.1111/1467-9574.00144.

Bailey T, Jain AK. 1978. A Note On Distance-Weighted k-Nearest Neighbor Rules. IEEE Trans Syst Man Cybern. 8:311–313. doi:10.5840/method1991918.

Birch CPD, Oom SP, Beecham JA. 2007. Rectangular and hexagonal grids used for observation, experiment and simulation in ecology. Ecol Modell. 206(3–4):347–359. doi:10.1016/j.ecolmodel.2007.03.041.

Blouin KD, Flannigan MD, Wang X, Kochtubajda B. 2016. Ensemble lightning prediction models for the province of Alberta, Canada. Int J Wildl Fire. 25(4):421–432. doi:10.1071/WF15111.

Bodzin AM, Anastasio D. 2006. Using Web-based GIS For Earth and Environmental Systems Education. J Geosci Educ. 54(3):295–300. doi:10.5408/1089-9995-54.3.295.

Bridge SRJ, Miyanishi K, Johnson EA. 2005. A critical evaluation of fire suppression effects in the boreal forest of Ontario. For Sci. doi:10.1093/forestscience/51.1.41.

Burrows WR, Kochtubajda B. 2010. A decade of cloud-to-ground lightning in Canada: 1999-2008. Part 1: Flash density and occurrence. Atmos - Ocean. 48(3):177–194. doi:10.3137/AO1118.2010.

Campos-Ruiz R, Parisien MA, Flannigan MD. 2018. Temporal patterns of wildfire activity in areas of contrasting human influence in the Canadian boreal forest. Forests. 9(4). doi:10.3390/f9040159.

Canadian Forest Service. 2020. CWFIS Datamart. Nat Resour Canada.

Chapin FS, McGuire AD, Ruess RW, Hollingsworth TN, Mack MC, Johnstone JF, Kasischke ES, Euskirchen ES, Jones JB, Jorgenson MT, et al. 2010. Resilience of Alaska's boreal forest to climatic change. Can J For Res. 40(7):1360–1370. doi:10.1139/X10-074.

Clarke PJ, Evans FC. 1954. Distance to Nearest Neighbor as a measure of spatial relationships in populations. Ecology. 35:445–453.

Cliff AD, Ord JK. 1981. Spatial and temporal analysis: autocorrelation in space and time. Quant Geogr a Br view.

Coogan S, Cai X, Jain P, Flannigan MD. 2018. Seasonality and trends in human- and lightning-caused wildfires ≥2 ha in Canada, 1959-2018. Int J Wildl Fire.:11–42.

Cooray V. 2014. The Lightning Flash. Second Edi. Technology TI of E and, editor. London.

Countryman CM. 1972. The fire environment concept - Pacific Southwest Forest and Range Experiment Station. In: The fire environment concept.

Cover TM, Hart PE. 1967. Nearest Neighbor. IEEE Trans Inf Theory. 13(1):21–27. doi:10.1007/978-0-387-35973-1_862.

Crisp MD, Burrows GE, Cook LG, Thornhill AH, Bowman DMJS. 2011. Flammable biomes dominated by eucalypts originated at the Cretaceous-Palaeogene boundary. Nat Commun. 2(1).

doi:10.1038/ncomms1191.

Delmelle E, Kim C, Xiao N, Chen W. 2013. Methods for space-time analysis and modeling: An overview. Int J Appl Geospatial Res. 4(4):1–18. doi:10.4018/jagr.2013100101.

Devillers R, Stein A, Bédard Y, Chrisman N, Fisher P, Shi W. 2010. Thirty Years of Research on Spatial Data Quality: Achievements, Failures, and Opportunities. Trans GIS. 14(4):387–400. doi:10.1111/j.1467-9671.2010.01212.x.

Dissing D, Verbyla DL. 2003. Spatial patterns of lightning strikes in interior Alaska and their relations to elevation and vegetation. Can J For Res. 33(5):770–782. doi:10.1139/x02-214.

Dixon PM. 2002. Ripley's K Function. Encycl Environmetrics. 3:1796–1803. doi:10.1002/9781118445112.stat07751.

Ebdon D. 1980. Nearest Neighbour Analysis in the Square Published by : The Royal Geographical Society (with the Institute of British Geographers) Linked references are available on JSTOR for this article : R Geogr Soc. 12(2):154–159.

ESRI. 2020. ArcGIS Desktop: Release 10.7. Redlands CA.

Fauria MM, Johnson EA. 2006. Large-scale climatic patterns control large lightning fire occurrence in Canada and Alaska forest regions. J Geophys Res Biogeosciences. 111(4). doi:10.1029/2006JG000181.

Flannigan MD, Stocks B, Wotton BM. 2000a. Climate change and forest fires. Sci Total Environ. 262(3):221–229. doi:10.1016/S0048-9697(00)00524-6.

Flannigan MD, Todd B, Wotton M, Stocks BJ. 2000b. Pacific Sea Surface Temperatures and

their relation to Area Burned in Canada Atmospheric Environment Service , Toronto , Ontario Faculty of Forestry , University ofToronto , Toronto , Ontario and Canadian forests a linkage may exist between the occurring.

Flannigan MD, Wotton BM. 1991. Lightning-ignited forest fires in northwestern Ontario. Can J Bot. 21:277–287.

Flannigan MD, Wotton BM, Marshall GA, de Groot WJ, Johnston J, Jurko N, Cantin AS. 2016. Fuel moisture sensitivity to temperature and precipitation: climate change implications. Clim Change. 134(1–2):59–71. doi:10.1007/s10584-015-1521-0.

Fuquay DM. 1982. Positive cloud-to-ground lightning in summer thunderstorms (Rocky Mountains). J Geophys Res. 87(C9):7131–7140. doi:10.1029/JC087iC09p07131.

Fuquay DM, Gaughman RG, Taylor AR, Hawe RG. 1967. Characteristics of Seven Lightning Discharges that Caused Forest Fires. J Geophys Res. 72(24):6371–6373.

Fuquay DM, Taylor AR, Hawe RG, Schmid Jr CW. 1972. Lightning Discharges that Caused Fores Fires. J Geophys Res. 77(12):1969–1971.

Gedalof Z, Peterson DL, Mantua NJ. 2005. Atmospheric, climatic, and ecological controls on extreme wildfire years in the Northwestern United States. Ecol Appl. 15(1):154–174. doi:10.1890/03-5116.

Genet H, McGuire AD, Barrett K, Breen A, Euskirchen ES, Johnstone JF, Kasischke ES, Melvin AM, Bennett A, Mack MC, et al. 2013. Modeling the effects of fire severity and climate warming on active layer thickness and soil carbon storage of black spruce forests across the landscape in interior Alaska. Environ Res Lett. 8(4). doi:10.1088/1748-9326/8/4/045016.

Genton MG, Butry DT, Gumpertz ML, Prestemon JP. 2006. Spatio-temporal analysis of wildfire ignitions in the St Johns River Water Management District, Florida. Int J Wildl Fire. 15(1):87–97. doi:10.1071/WF04034.

Gillett NP, Weaver AJ, Zwiers FW, Flannigan MD. 2004. Detecting the effect of climate change on Canadian forest fires. Geophys Res Lett. 31(18). doi:10.1029/2004GL020876.

Government of Alberta. 2020. Alberta Wildfire. [accessed 2020 Sep 5]. https://wildfire.alberta.ca/.

Government of British Columbia. 2020. Wildfire Season Summary. [accessed 2020 Sep 5]. https://www2.gov.bc.ca/gov/content/safety/wildfire-status/about-bcws/wildfire-history/wildfire-season-summary.

Hamed KH. 2009. Exact distribution of the Mann-Kendall trend test statistic for persistent data. J Hydrol. 365(1–2):86–94. doi:10.1016/j.jhydrol.2008.11.024. http://dx.doi.org/10.1016/j.jhydrol.2008.11.024.

Hanes CC, Wang X, Jain P, Parisien MA, Little JM, Flannigan MD. 2019. Fire-regime changes in canada over the last half century. Can J For Res. 49(3):256–269. doi:10.1139/cjfr-2018-0293.

Hart SJ, Henkelman J, McLoughlin PD, Nielsen SE, Truchon-Savard A, Johnstone JF. 2019. Examining forest resilience to changing fire frequency in a fire-prone region of boreal forest. Blackwell Publishing Ltd.

He T, Pausas JG, Belcher CM, Schwilk DW, Lamont BB. 2012. Fire-adapted traits of Pinus arose in the fiery Cretaceous. New Phytol. 194(3):751–759. doi:10.1111/j.1469-8137.2012.04079.x.

Hileman AR. 1999. Insulation Coordination for Power Systems. IEEE Power Eng Rev. 19(9):43. doi:10.1109/MPER.1999.785802.

IUCN. 1990. 18th General Assembly. In: Global Climate Change. p. 1–2.

Jain P, Wang X, Flannigan MD. 2017. Trend analysis of fire season length and extreme fire weather in North America between 1979 and 2015. Int J Wildl Fire. 26(12):1009–1020. doi:10.1071/WF17008.

Jenness J. 2012. Repeating shapes for ArcGIS: Jenness Enterprises.

Johnston LM, Flannigan MD. 2018. Mapping Canadian wildland fire interface areas. Int J Wildl Fire. 27(1):1–14. doi:10.1071/WF16221.

Kasischke ES, Verbyla DL, Rupp TS, McGuire AD, Murphy KA, Jandt R, Barnes JL, Hoy EE, Duffy PA, Calef M, et al. 2010. Alaska's changing fire regime - implications for the vulnerability of its boreal forests. Can J For Res. 40(7):1313–1324. doi:10.1139.

Kilinc M, Beringer J. 2007. The spatial and temporal distribution of lightning strikes and their relationship with vegetation type, elevation, and fire scars in the northern Territory. J Clim. 20(7):1161–1173. doi:10.1175/JCLI4039.1.

Kochtubajda B, Burrows WR. 2010. A decade of cloud-to-ground lightning in Canada: 1999-2008. Part 2: Polarity, multiplicity and first-stroke peak current. Atmos - Ocean. 48(3):195–209. doi:10.3137/AO1119.2010.

Krawchuk MA, Cumming SG, Flannigan MD, Wein RW. 2006. Biotic and abiotic regulation of lightning fire initiation in the mixedwood boreal forest. Ecology. 87(2):458–468. doi:10.1890/05-1021.

Larjavaara M, Kuuluvainen T, Rita H. 2005. Spatial distribution of lightning-ignited forest fires in Finland. For Ecol Manage. 208(1–3):177–188. doi:10.1016/j.foreco.2004.12.005.

Latham D, Williams E. 2001. Lightning and Forest Fires in California. In: Forest Fires. p. 375–418.

Liu W, Li X. 2016. Life cycle characteristics of warm-season severe Thunderstorms in Central United States from 2010 to 2014. Climate. 4(3):1989–1998. doi:10.3390/cli4030045.

Lloyd CD. 2014. Chapter 3: The modifiable areal unit problem. In: Exploring Spatial Scale in Geography. p. 29–44.

Magnussen S, Taylor SW. 2012. Inter- and intra-annual profiles of fire regimes in the managed forests of Canada and implications for resource sharing. Int J Wildl Fire. doi:10.1071/WF11026.

Malanson GP. 1987. Diversity, stability, and resilience: effects of fire regime. In The role of fire in ecological systems. Trabaud L, editor. SPB Academic Publishing by, The Hague.

Mann HB. 1945. Nonparametric Tests Against Trend. Econometriica. 13(3):245–259.

Masrur A, Petrov AN, DeGroote J. 2018. Circumpolar spatio-temporal patterns and contributing climatic factors of wildfire activity in the Arctic tundra from 2001-2015. Environ Res Lett. 13(1). doi:10.1088/1748-9326/aa9a76.

Merrill DF, Alexander ME. 1987. Glossary of Forest Fire Management Terms. 4th ed.

Meyer VK, Höller H, Betz HD. 2013. The temporal evolution of three-dimensional lightning parameters and their suitability for thunderstorm tracking and nowcasting. Atmos Chem Phys. 13(10):5151–5161. doi:10.5194/acp-13-5151-2013.

Meyn A, Taylor SW, Flannigan MD, Thonicke K, Cramer W. 2010. Relationship between fire, climate oscillations, and drought in British Columbia, Canada, 1920-2000. Glob Chang Biol. 16(3):977–989. doi:10.1111/j.1365-2486.2009.02061.x.

Mitsopoulos I, Mallinis G, Karali A, Giannakopoulos C, Arianoutsou M. 2016. Mapping fire behaviour under changing climate in a Mediterranean landscape in Greece. Reg Environ Chang. 16(7):1929–1940. doi:10.1007/s10113-015-0884-0.

Moran PAP. 1950. Notes on Continuous Stochastic Phenomena. Biometrika. doi:10.2307/2332142.

Morissette J, Gauthier S. 2008. Study of cloud - to - ground lightning in Quebec : 1996 – 2005. Atmos - Ocean. 46(4):443–454. doi:10.3137/AO919.2008.

Moritz MA, Morais ME, Summerell LA, Carlson JM, Doyle J. 2005. Wildfires, complexity, and highly optimized tolerance. Proc Natl Acad Sci U S A. 102(50):17912–17917. doi:10.1073/pnas.0508985102.

Mundo IA, Wiegand T, Kanagaraj R, Kitzberger T. 2013. Environmental drivers and spatial dependency in wildfire ignition patterns of northwestern Patagonia. J Environ Manage. 123:77–87. doi:10.1016/j.jenvman.2013.03.011. http://dx.doi.org/10.1016/j.jenvman.2013.03.011.

Oberle M. 1969. Forest Fires : Suppression Policy Has Its Ecological Drawbacks. Science (80-). 165(3893):568–571.

Openshaw S. 1977. A Geographical Solution to Scale and Aggregation Problems in Region-Building, Partitioning and Spatial Modelling. Trans Inst Br Geogr. 2(4):459. doi:10.2307/622300.

Openshaw S, Taylor PJ. 1979. A million or so correlation coefficients: three experiments on the modifiable areal unit problem. Stat Appl Spat Sci.

Ord JK, Getis A. 1995. Local Spatial Autocorrelation Statistics: Distributional Issues and an Application. Geogr Anal. 27(4):A3288–A3288. doi:10.1164/ajrccm-conference.2010.181.1_meetingabstracts.a3288.

Ordóñez C, Saavedra A, Rodríguez-Pérez JR, Castedo-Dorado F, Covián E. 2012. Using model-based geostatistics to predict lightning-caused wildfires. Environ Model Softw. 29(1):44–50. doi:10.1016/j.envsoft.2011.10.004.

Orville RE, Huffines GR, Burrows WR, Holle RL, Cummins KL. 2002. The North American lightning detection network (NALDN) - first results: 1998-2000. Mon Weather Rev. 130(8):2098–2109. doi:10.1175/1520-0493(2002)130<2098:TNALDN>2.0.CO;2.

Parisien MA, Parks SA, Krawchuk MA, Flannigan MD, Bowman LM, Moritz MA. 2011. Scale-dependent controls on the area burned in the boreal forest of Canada, 1980-2005. Ecol Appl. 21(3):789–805. doi:10.1890/10-0326.1.

Parisien MA, Peters VS, Wang Y, Little JM, Bosch EM, Stocks BJ. 2006. Spatial patterns of forest fires in Canada, 1980-1999. Int J Wildl Fire. 15(3):361–374. doi:10.1071/WF06009.

Pausas JG, Keeley JE. 2014. Evolutionary ecology of resprouting and seeding in fire-prone ecosystems. New Phytol. 204(1):55–65. doi:10.1111/nph.12921.

Pearson SM. 1993. The spatial extent and relative influence of landscape-level factors on wintering bird populations. Landsc Ecol. 8(1):3–18. doi:10.1007/BF00129863.

Pinder D, Shimada I, Gregory D. 1979. The Nearest-Neighbor Staistic: Archaeological

application and new developments. Am Antiq. 44(3):430–445.

Podur J, Martell DL, Csillag F. 2003. Spatial patterns of lightning-caused forest fires in Ontario, 1976-1998. Ecol Modell. 164(1):1–20. doi:10.1016/S0304-3800(02)00386-1.

Portier J, Gauthier S, Bergeron Y. 2019. Spatial distribution of mean fire size and occurrence in eastern Canada : influence of climate , physical environment and lightning strike density. Int J Wildl Fire.

Price C, Rind D. 1994. The Impact of a 2 × CO 2 Climate on Lightning-Caused Fires . J Clim. 7(10):1484–1494. doi:10.1175/1520-0442(1994)007<1484:tioacc>2.0.co;2.

Pyne SJ, Andrews PA, Laven RD. 1996. Introduction to Wildland Fire. New York: Wiley.

Radeloff VC, Hammer RB, Stewart S, Fried JS, Holcomb SS, McKeefry JF. 2005. The Wildland Urban Interface in America. Ecol Appl. 15(3):799–805.

Reap RM. 1991. Climatological Characteristics and Objective Prediction of Thunderstorms over Alaska. Weather Forecast. 6(3):309–319. doi:10.1175/1520-0434(1991)006<0309:ccaopo>2.0.co;2.

Renkin R, Despain D. 1991. Fuel moisture, forest type and lightning-cause fire in Yellowstone National Park. Can J For Res. 22:37–45.

Robinne FN, Parisien MA, Flannigan MD. 2016. Anthropogenic influence on wildfire activity in Alberta, Canada. Int J Wildl Fire. 25(11):1131–1143. doi:10.1071/WF16058.

Robinson WS. 1950. Ecological Correlations and the Behavior of Individuals. Am Sociol Rev. 15(3):351–357. https://www.jstor.org/stable/2087176.

Rodrigues M, Costafreda-Aumedes S, Comas C, Vega-García C. 2019. Spatial stratification of wildfire drivers towards enhanced definition of large-fire regime zoning and fire seasons. Sci Total Environ. 689:634–644. doi:10.1016/j.scitotenv.2019.06.467.

Romps DM, Seeley JT, Vollaro D, Molinari J. 2014. Projected increase in lightning strikes in the united states due to global warming. Science (80-). 346(6211):851–854. doi:10.1126/science.1259100.

Rowe JS. 1983. Concepts of Fire Effects on Plant Individuals and Species. Role Fire North Circumpolar Ecosyst.(1973):135–154.

Rowe JS, Scotter GW. 1973. Fire in the boreal forest. Quat Res. 3(3):444–464. doi:10.1016/0033-5894(73)90008-2.

Saba MMF, Pinto Jr O, Ballarotti MG. 2006. Relation between lightning return stroke peak current and following continuing current. Geophys Res Lett. 33(23). doi:10.1029/2006GL027455.

Schuur EAG, Abbott BW, Bowden WB, Brovkin V, Camill P, Canadell JG, Chanton JP, Chapin FS, Christensen TR, Ciais P, et al. 2013. Expert assessment of vulnerability of permafrost carbon to climate change. Clim Change. 119(2):359–374. doi:10.1007/s10584-013-0730-7.

Shimazaki H, Shinomoto S. 2007. A method for selecting the bin size of a time histogram. Neural Comput. doi:10.1162/neco.2007.19.6.1503.

Sommers WT, Coloff SG, Conard SG. 2011. Chapter 3: Fire Regimes. In: JFSP Synthesis Reports. Paper 19. p. 27–41. http://www.firescience.gov/JFSP_fire_history.cfm.

Stocks BJ, Lawson BD, Alexander ME, Van Wagner CE, McAlpine RS, Lynham TJ, Dube DE.

1989. Canadian Forest Fire Danger Rating System: an overview. For Chron. 65:258–265. doi:doi:10.5558/tfc65258-4.

Stocks BJ, Martell DL. 2016. Forest fire management expenditures in Canada: 1970-2013. For Chron. 92(3):298–306. doi:10.5558/tfc2016-056.

Stocks BJ, Mason JA, Todd JB, Bosch EM, Wotton BM, Amiro BD, Flannigan MD, Hirsch KG, Logan KA, Martell DL, et al. 2003. Large forest fires in Canada, 1959-1997. J Geophys Res D Atmos. 108(1). doi:10.1029/2001JD000484.

Taylor SW, Pike RG, Alexander ME. 1996. Field guide to the Canadian Forest Fire Behavior Prediction (FBP) system. Can For Serv.

Team Rs. 2005. RStudio: Integrated Development for R studio Inc. R Beginners.

Terrell GR, Scott DW. 1985. Oversmoothed nonparametric density estimates. J Am Stat Assoc. doi:10.1080/01621459.1985.10477163.

The Conference Board of Canada. 2017. Fort McMurray Wildfires: Assessing the Economic Impacts. https://www.conferenceboard.ca/reports/briefings/alberta-wildfires.aspx.

Thom D, Seidl R. 2016. Natural disturbance impacts on ecosystem services and biodiversity in temperate and boreal forests. Biol Rev Camb Philos Soc. 91(3):760–781. doi:10.1111/brv.12193.

Turetsky MR, Baltzer JL, Johnstone JF, Mack MC, McCann K, Schuur EAG. 2017. Losing Legacies, Ecological Release, and Transient Responses: Key Challenges for the Future of Northern Ecosystem Science. Ecosystems. 20(1):23–30. doi:10.1007/s10021-016-0055-2.

Turetsky MR, Benscoter B, Page S, Rein G, Van Der Werf GR, Watts A. 2015. Global

vulnerability of peatlands to fire and carbon loss. Nat Geosci. 8(1):11–14. doi:10.1038/ngeo2325. http://dx.doi.org/10.1038/ngeo2325.

Turner MG, Gardner RH, O'Niell R V. 2001. Landscape Ecology in Theory and Practice. New York, NY: Springer US.

Uman MA. 1985. Lightning return stroke electric and magnetic fields. J Geophys Res. 90(D4):6121–6130. doi:10.1029/JD090iD04p06121.

Vant-Hull B, Thompson T, Koshak W. 2018. Optimizing Precipitation Thresholds for Best Correlation Between Dry Lightning and Wildfires. J Geophys Res Atmos. 123(5):2628–2639. doi:10.1002/2017JD027639.

Vázquez A, Moreno JM. 1993. Sensitivity of fire occurrence to meteorological variables in Mediterranean and Atlantic areas of Spain. Landsc Urban Plan. 24(1–4):129–142. doi:10.1016/0169-2046(93)90091-Q.

Vázquez A, Moreno JM. 1998. Patterns of lightning-, and people-caused fires in Peninsular Spain. Int J Wildl Fire. 8(2):103–115. doi:10.1071/WF9980103.

Vázquez A, Moreno JM. 2001. Spatial distribution of forest fires in Sierra de Gredos (Central Spain). For Ecol Manage. 147(1):55–65. doi:10.1016/S0378-1127(00)00436-9.

Veraverbeke S, Rogers BM, Goulden ML, Jandt RR, Miller CE, Wiggins EB, Randerson JT. 2017. Lightning as a major driver of recent large fire years in North American boreal forests. Nat Clim Chang. 7(7):529–534. doi:10.1038/nclimate3329.

Van Wagner CE. 1987. Development and structure of the Canadian forest fire weather index system.

Wagner VCE. 1977. Conditions for the start and spread of crown fire. Can J For Res. 7:23–34.

Van Wagtendonk JW. 1993. Spatial analysis of lightning strikes in Yosemite National Park. In: Proceedings of the 11th conference on fire and forest meteorology. p. 605–611.

Van Wagtendonk JW, Cayan DR. 2010. Temporal and Spatial Distribution of Lightning Strikes in California in Relation To Large-scale Weather Patterns. Fire Ecol. 4(1):34–56. doi:10.4996/fireecology.0401034.

Van Wagtendonk K, David B. 2009. Spatial patterns of lightning strikes and fires in Yosemite National Park. Pap Present 12th Conf Fire For Meteorol Oct 1993, Jekyll Island, GA.:125–130.

Wang X, Thompson DK, Marshall GA, Tymstra C, Carr R, Flannigan MD. 2015. Increasing frequency of extreme fire weather in Canada with climate change. Clim Change. 130(4):573–586. doi:10.1007/s10584-015-1375-5.

Wang Y, Anderson KR. 2010. An evaluation of spatial and temporal patterns of lightning- and human-caused forest fires in Alberta, Canada, 1980-2007. Int J Wildl Fire. 19(8):1059–1072. doi:10.1071/WF09085.

Weber MG, Flannigan MD. 1997. Canadian boreal forest ecosystem structure and function in a changing climate: Impact on fire regimes. Environ Rev. 5(3–4):145–166. doi:10.1139/a97-008.

Weber MG, Stocks BJ. 1998. Forest fires and sustainability in the boreal forests of Canada. Ambio. 27(7):545–550.

Whitman E, Batllori E, Parisien MA, Miller C, Coop JD, Krawchuk MA, Chong GW, Haire SL. 2015. The climate space of fire regimes in north-western North America. J Biogeogr. 42(9):1736–1749. doi:10.1111/jbi.12533.

Wierzchowski J, Heathcott M, Flannigan MD. 2002. Lightning and lightning fire, central cordillera, Canada. Int J Wildl Fire. 11(1):41–51. doi:10.1071/WF01048.

Wotton BM, Flannigan MD. 1993. Length of the fire season in a changing climate. For Chron. doi:10.5558/tfc69187-2.

Wotton BM, Flannigan MD, Marshall GA. 2017. Potential climate change impacts on fire intensity and key wildfire suppression thresholds in Canada. Environ Res Lett. 12(9). doi:10.1088/1748-9326/aa7e6e.

Wotton BM, Nock CA, Flannigan MD. 2010. Forest fire occurrence and climate change in Canada. Int J Wildl Fire. 19(3):253–271. doi:10.1071/WF09002.